

# Discovery of DDO-2213 as a Potent and Orally Bioavailable Inhibitor of the WDR5–Mixed Lineage Leukemia 1 Protein–Protein Interaction for the Treatment of MLL Fusion Leukemia

Published as part of the Journal of Medicinal Chemistry special issue “Epigenetics 2022”.

Weilin Chen,<sup>▽</sup> Xin Chen,<sup>▽</sup> Dongdong Li, Jianrui Zhou, Zhengyu Jiang,\* Qidong You,\* and Xiaoke Guo\*

 Cite This: *J. Med. Chem.* 2021, 64, 8221–8245

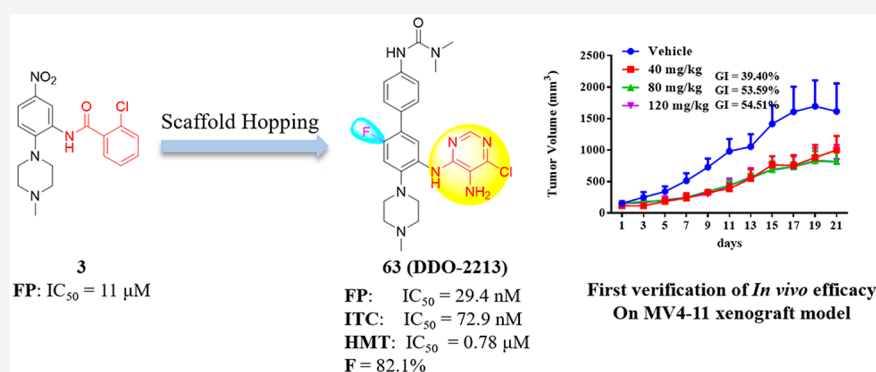
 Read Online

ACCESS |

 Metrics & More

 Article Recommendations

 Supporting Information



**ABSTRACT:** WD repeat-containing protein 5 (WDR5) is essential for the stability and methyltransferase activity of the mixed lineage leukemia 1 (MLL1) complex. Dysregulation of the *MLL1* gene is associated with human acute leukemias, and the direct disruption of the WDR5–MLL1 protein–protein interaction (PPI) is emerging as an alternative strategy for MLL-rearranged cancers. Here, we represent a new aniline pyrimidine scaffold for WDR5–MLL1 inhibitors. A comprehensive structure–activity analysis identified a potent inhibitor **63 (DDO-2213)**, with an IC<sub>50</sub> of 29 nM in a competitive fluorescence polarization assay and a *K<sub>d</sub>* value of 72.9 nM for the WDR5 protein. Compound **63** selectively inhibited MLL histone methyltransferase activity and the proliferation of MLL translocation-harboring cells. Furthermore, **63** displayed good pharmacokinetic properties and suppressed the growth of MV4-11 xenograft tumors in mice after oral administration, first verifying the *in vivo* efficacy of targeting the WDR5–MLL1 PPI by small molecules.

## INTRODUCTION

WDR5, a member of the WD40 repeat protein family,<sup>1,2</sup> functions as a critical scaffolding component in numerous protein complexes that relate epigenetic machinery and transcriptional regulation.<sup>3</sup> WDR5 is comprised of a circular seven-bladed β-propeller fold where each blade interconnects through four-stranded antiparallel β-sheets, which generally mediate protein–protein interactions (PPIs).<sup>1–4</sup> WDR5 has two major binding sites: WDR5 binding motif (WBM) and WDR5 interaction motif (WIN) sites.<sup>5–11</sup> The most well-studied role of WDR5 is the formation of MLL/SET (MLL1–4, SET1A, and SET1B) complexes via the WIN site.<sup>12</sup> In these complexes, MLL1 and WDR5 PPI are uniquely required for MLL1 histone methyltransferase activity. In addition, MLL1 regulates gene transcription by mediating the monomethylation, dimethylation, and trimethylation of histone 3 lysine 4 (H3K4).<sup>13,14</sup> However, this enzymatic activity is relatively

weak when it is present in isolation, and the constitution of the MLL core complex (MLL1, WDR5, ASH2L, RbBP5, and DPY-30) dramatically enhances the enzymatic activity.<sup>15</sup> Among these interactions, the WDR5–MLL1 interaction is necessary for the stability and H3K4 HMT activity of MLL1. The chromosomal translocation of an allele in the 11q23 *MLL1* gene to one of over 70 different partner genes causes a unique group of leukemias with poor prognoses and treatment outcomes.<sup>16</sup> It has been reported that 70% of infant acute lymphoid leukemia (ALL) cases and 5–10% of adult acute

Received: January 19, 2021

Published: June 9, 2021



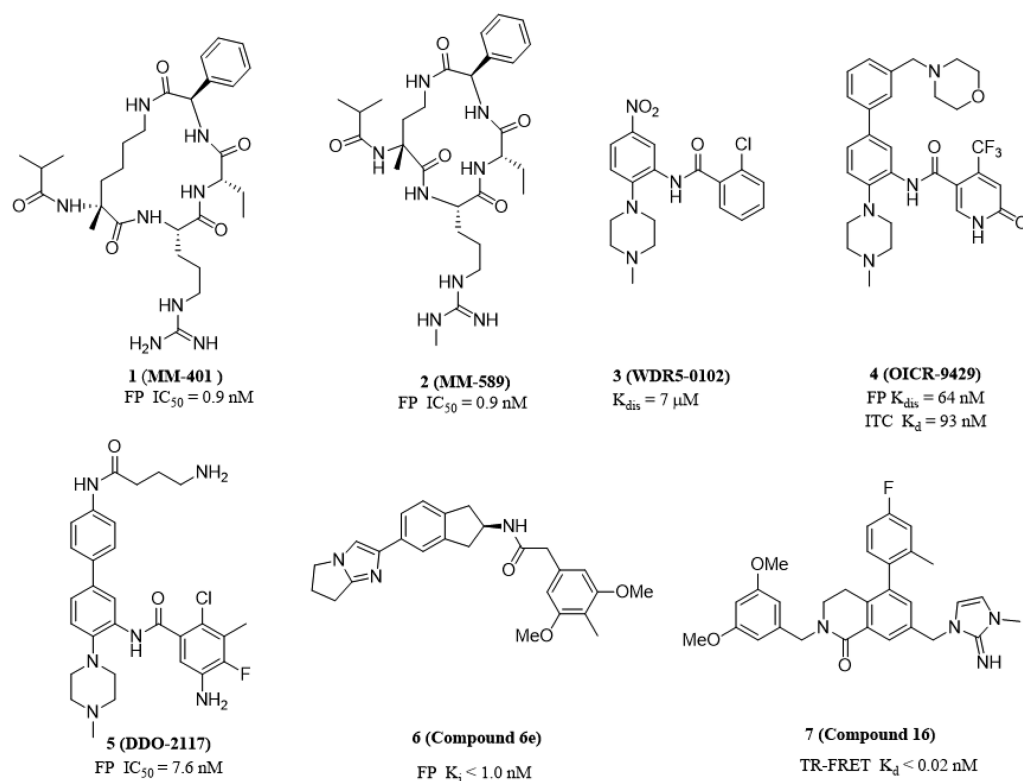


**Figure 1.** Representative peptidomimetic and nonpeptide inhibitors of the WDR5 WIN-site.

myeloid leukemia (AML) cases are associated with MLL rearrangements, such as MLL–AF4, MLL–AF9, and MLL–ENL.<sup>17–19</sup> However, the lack of a C-terminal catalytic SET domain in MLL fusion proteins leads to the loss of their histone methyltransferase activity. Interestingly, the synergy between the remaining wild-type MLL allele and the MLL fusion allele is necessary for leukemogenesis.<sup>14,19</sup> Therefore, targeting the MLL1–WDR5 PPI is considered to be an effective strategy for the treatment of leukemia containing MLL fusion proteins (Figure S1).<sup>13–22</sup>

Because the interaction of WDR5–MLL1 is important for the MLL1 complex, various WDR5–MLL1 PPI antagonists, including peptides and small molecules, have been discovered, and the four representative types of WDR5 WIN site inhibitors that disrupt this interaction are shown in Figure 1. Peptidomimetic compounds with sub-nanomolar affinities to the WDR5 protein, low-nanomolar inhibitions of MLL1 enzyme catalytic activity, and antiproliferative activity in cells, such as MM-401 (**1**) and MM-589 (**2**), were obtained by imitating the MLL peptide residues.<sup>23–26</sup> The first nonpeptide class of small-molecule antagonists (WDR5–0102, **3**) was identified by the high-throughput screening of a compound library.<sup>27</sup> According to the cocrystal structures of WDR5 inhibitors, several more potent small molecules were obtained in the subsequent optimization, such as OICR-9429 (**4**) with a high affinity to the WDR5 protein ( $IC_{50} = 64$  nM) and the favorable antiproliferative activity of human C/EBP $\alpha$  mutant AML cells.<sup>28,29</sup> We previously reported that DDO-2117 (**5**) disturbed the WDR5–MLL1 interaction ( $IC_{50} = 7.6$  nM) *in vitro*.<sup>30</sup> Recently, the third class of representative small molecules, **6e** (**6**), was discovered by NMR-based fragment screening, displaying a remarkable affinity to the WDR5 protein ( $K_i < 1$  nM).<sup>31</sup> The fourth class of representative small molecules, compound **16** (**7**) containing a dihydroisoquinolin-

none bicyclic core, showed a picomolar binding affinity and inhibited the proliferation of MYC-driven cancer cells.<sup>32,33</sup> In conclusion, these studies suggest that the WDR5 protein, especially the WIN site, could be a promising anticancer target and promote the further study of new inhibitors.

Here, we describe the design and synthesis of a series of new aminopyrimidine-based WDR5–MLL1 PPI inhibitors and discuss the structure–activity relationship (SAR). The represented compound **63** showed tight binding to the WDR5 protein ( $K_d = 72.99$  nM) *in vitro*, selectively inhibited the HMT activity of MLL1 both *in vitro* and in cells, effectively reduced MLL fusion-protein-dependent gene expressions, and selectively restrained the proliferation of leukemia cells harboring MLL fusion proteins (MLL-FPs) with little toxicity to non-MLL cells. Moreover, compound **63** showed favorable drug-like properties and exhibited obvious anticancer effects in the MLL fusion leukemia MV4-11 xenografts after oral administration. This research not only reports a potent and orally bioavailable WDR5–MLL1 inhibitor with a novel aminopyrimidine scaffold but also is the first to show the therapeutic potential of small-molecule WDR5–MLL1 inhibitors against MLL fusion leukemia *in vivo*.

## RESULTS AND DISCUSSION

**Discovery of Initial Hit Compound 9 as a WDR5–MLL1 Inhibitor.** Targeting a protein–protein interaction is an emerging strategy for drug design.<sup>34–38</sup> For the WDR5–MLL1 PPI, the MLL1 binding site in the WDR5 domain is a well-defined cavity. In an effort to discover a new scaffold for WDR5–MLL1 inhibitors, we pursued a scaffold-hopping approach utilizing the structural information on reported inhibitor binding to the WDR5 protein to identify a novel hit. We observed the cocrystal structure between WDR5 and compound **3** (PDB 3SMR), the first WDR5 WIN site small-

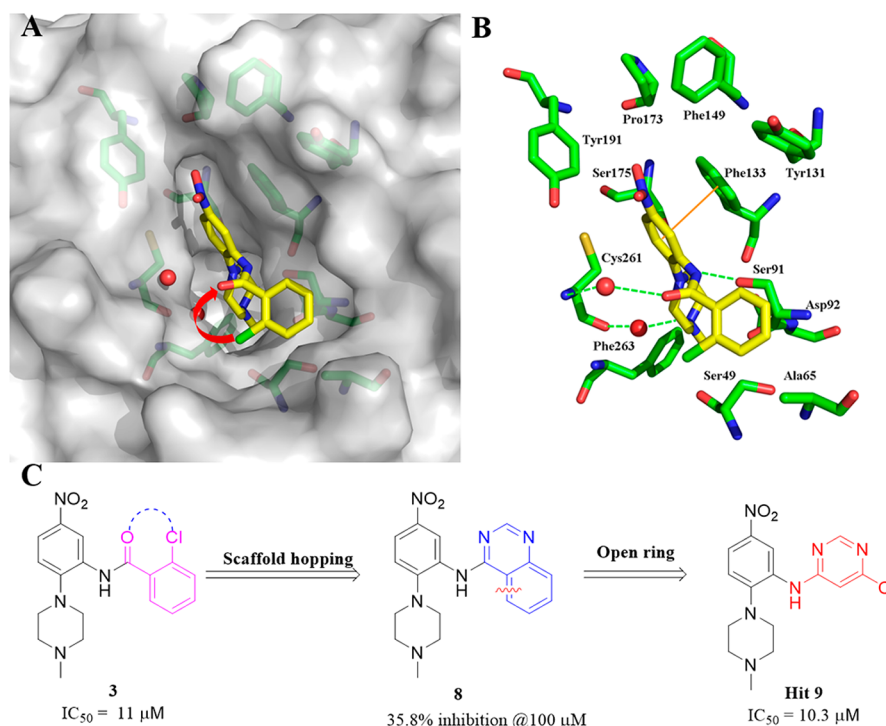


**Figure 2.** (A) Cocystal structure of compound 3 with WDR5 (PDB 3SMR). (B) Binding mode of compound 3 (yellow) with the key residues (green) in the WDR5 WIN site (PDB 3SMR). (C) The design of hit compound 9.

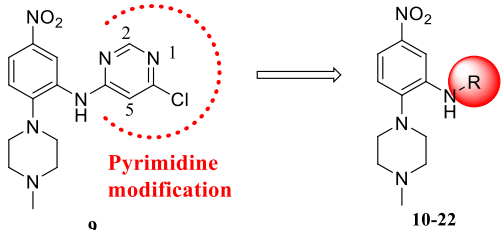
molecule inhibitor, and found that the O atom of the amide and the Cl atom of the benzene ring were on the same side. Simultaneously, considering the contributions of the O atom to the binding activity via the formation of a water-mediated hydrogen bond with the backbone nitrogen of Cys261 (Figure 2A, 2B), we supposed that the cyclization of the O atom with the Cl moiety may result in a conformational restriction, producing compound 8 (Figure 2C). Compound 8 showed weak inhibitory activity against the WDR5–MLL1 PPI as determined by a fluorescence polarization (FP) assay (35.8% inhibition at 100  $\mu M$ ).<sup>25</sup> We speculated that the volume of the quinoline ring was too large to extend well into the hydrophobic cavity, formed by Leu321, Ala65, Ser49, and Ser91, resulting in the dramatically decreased activity. Following a reduction in the molecular rigidity, compound 9 was obtained by opening the quinoline ring, which showed an activity equivalent to that of 3 (as assessed by an FP assay,  $IC_{50} = 10.3 \mu M$ ) (Figure 2C). This starting compound represents a new scaffold for WDR5 inhibition and deserves further optimization.

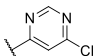
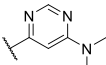
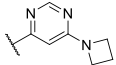
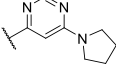
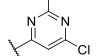
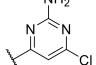
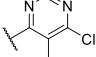
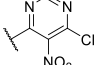
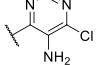
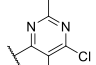
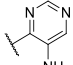
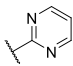
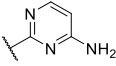
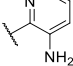
**SAR of the Pyrimidine Ring.** To improve the WDR5–MLL1 inhibitory potency, we explored the effects of the pyrimidine ring by including various substituents on the pyrimidine ring in compound 9 and changing the pyrimidine ring, as shown in Table 1. First, the chloro group was replaced by different secondary amines, which resulted in target compounds 10–12. These analogues gave the abolished activity. Therefore, we decided to preserve the original chloro group to synthesize the subsequent analogues. We then introduced methyl, amino, and nitro groups at different positions around the pyrimidine ring, and compounds 13–18 were obtained. The inhibition activity of compounds with substitutions at the 2-position (13 and 14) dramatically decreased. Compounds with a methyl (15) or nitro (16) substitution at the 5-position were also not ideal, while the

amino substituent (17) at the 5-position gave about a fourfold increase in inhibitory activity. In addition, the decreased inhibitory activity of compound 18 again demonstrated that the 2-position was not suitable for substitution. Compound 19, which removed the chloro atom from compound 17, also showed a dramatic loss of activity. Replacing the 4-chloro-substituted pyrimidine ring with several heterocycles also failed to produce active compounds (20–22). Thus, 17 contained the most suitable group for the optimization of the pyrimidine moiety due to its favorable inhibitory activity, indicating that the 6-chloro-5-aminopyrimidine group was essential for the inhibitory activity.

To investigate the binding mode of this chemotype with the WDR5 protein, a molecular docking study was performed utilizing DS 3.0 for the most potent compound 17. The binding mode showed that 17 can insert into the arginine-binding pocket at the central cavity (Figure 3A). The *N*-methylpiperazine moiety was also anchored at the bottom of the pocket and formed a water-mediated hydrogen bond with the backbone carbonyl of Cys261. The 6-chloro-5-aminopyrimidine group lay in a hydrophobic and shallow cavity surrounded by Ala47, Ser49, Ala65, Ser91, Ile305, and Leu321. The core phenyl ring formed a  $\pi$ – $\pi$  stack interaction with Phe133. As expected, the nitrogen atom at the 3-position of the pyrimidine formed a water-mediated hydrogen bond with the backbone nitrogen of Cys261, which was a similar interaction to that observed with the amide group of the benzamide compound 3. Further, the amino group of the aniline formed a direct hydrogen bond with the side chain of Ser91. Moreover, the newly introduced amino group on the pyrimidine ring can form a direct hydrogen bond interaction with Asp107, which may be the reason for the increased potency of 17 compared to that of 9 (Figure 3A). Then, we explored the SAR of 17 around three parts, including the *N*-methylpiperazine substituents (exhibiting a potential space to

Table 1. Effects of Pyrimidine Ring Modifications on WDR5–MLL1 Inhibition



Compd.	R	FP IC <sub>50</sub> (μM) <sup>a</sup>
9		10.3 ± 0.42
10		>50
11		>50
12		>50
13		>50
14		20.4 ± 1.0
15		>50
16		>50
17		2.66 ± 0.37
18		12.1 ± 0.55
19		>50
20		>50
21		>50
22		>50

<sup>a</sup>IC<sub>50</sub> values represent the mean ± SD of three independent experiments.

form polar and  $\pi$ – $\pi$  stack interactions), the nitro substituent (which is surrounded by hydrophobic residues involving Phe133, Phe149, Pro173, and Tyr191 and is closed to the protein surface), and the core phenyl substituents (Figure 3B).

**SAR of the *N*-Methylpiperazine Substituent.** On the one hand, the docking study showed the available space and possibility of hydrogen bond formation with Asp92 in addition to the  $\pi$ – $\pi$  stack interaction formation with Phe263 at the

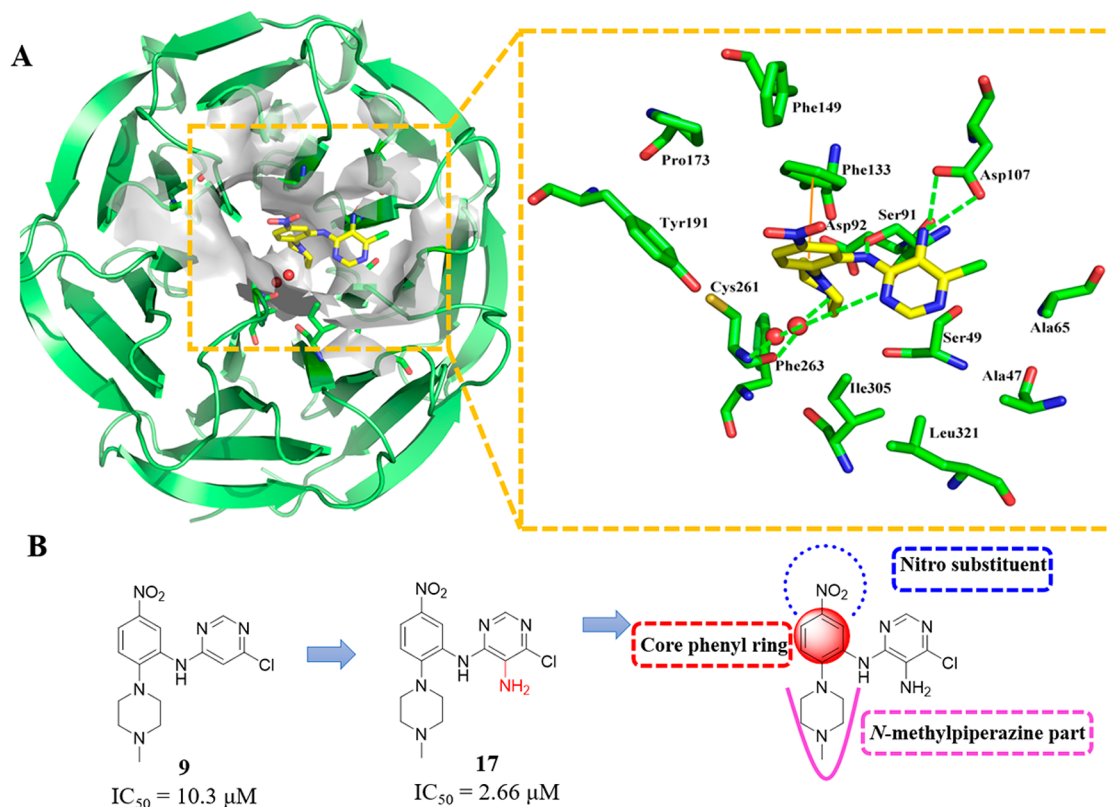


**Figure 3.** (A) Proposed binding modes showing the structures of 17 docked into WDR5 (PDB 4QL1). The green dashed lines represent hydrogen bonds, and the orange lines represent  $\pi$ – $\pi$  stacking interactions. (B) The optimization of compound 17.

**Table 2.** Effects of *N*-Methylpiperazine Region Modifications on WDR5–MLL1 Inhibition

Compd.	R	FP $IC_{50}$ ( $\mu M$ ) <sup>a</sup>
23		45.1 ± 1.4
24		> 50
25		38.1 ± 0.96
26		>50
27		>50
28		>50

<sup>a</sup> $IC_{50}$  values represent the mean ± SD of three independent experiments.

bottom of the arginine-binding cleft (Figure 3). On the other hand, the structural features of 17 may be different from those of the benzamide compound 3. Therefore, we further tried to

investigate the *N*-methylpiperazine substituents of 17. Different amines were introduced to this region to obtain the analogs listed in Table 2. Unfortunately, all the compounds with *N*-

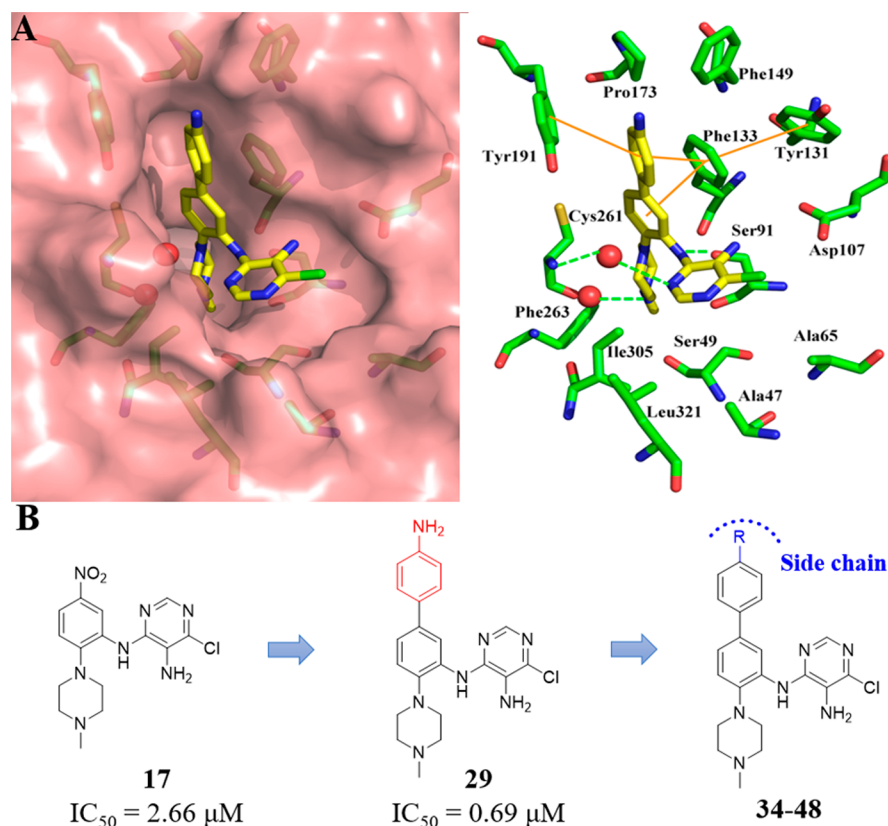


Table 3. Effects of Nitro Substituents on WDR5–MLL1

17 29-33

Compd.	R	FP IC <sub>50</sub> (μM) <sup>a</sup>
29		0.690 ± 0.11
30		1.56 ± 0.23
31		5.71 ± 0.13
32		11.4 ± 0.87
33		0.860 ± 0.070

<sup>a</sup>IC<sub>50</sub> values represent the mean ± SD of three independent experiments.



**Figure 4.** (A) Proposed binding modes showing the structures of **29** docked into WDR5 (PDB 4QL1). The green dashed lines represent the hydrogen bonds, and the orange lines represent the  $\pi$ - $\pi$  stacking interactions. (B) The optimization of compound **29** and design of **34–48**.

methylpiperazine modifications had lower or no activities, including demethylated compounds (**23**), compounds with a

morpholine replacement (**24**), and *N*-ethylation (**25**), *N*-cyclopropanation (**26**), *N*-hydroxyethyl (**27**), and *N*-phenyl

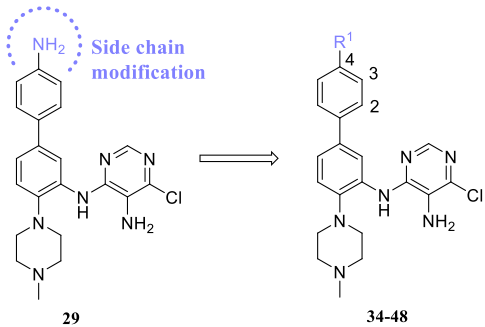
(28) modifications of the piperazine ring. These results further emphasized the importance of the conformational and steric constraints of the methylpiperazine moiety. Therefore, we opted to retain the *N*-methylpiperazine moiety and chose 17 for further optimization.

**SAR of the Nitro Substituent.** A subsequent SAR optimization was conducted to the focus on the nitro group of 17. Previous SAR studies at this position showed that the introduction of an aromatic ring formed van der Waals interactions with Phe133, Phe149, Pro173, and Tyr191 and led to favorable improvements in potency.<sup>29,30,39,40</sup> We thought that this moiety deserved to be broadly explored to capture the aforementioned interactions with nearby residues. To this end, we introduced benzene rings and different aromatic heterocycles via Suzuki coupling reactions. The SAR data of these compounds are summarized in Table 3. The introduction of benzene rings (29 and 30) improved the potency relative to that of 17, and 29 (with a 4-amino phenyl substituent) showed a greater inhibition than 30 (with a 4-methoxy phenyl substituent), suggesting that hydrophilic substituents at the 4-position of the newly introduced phenyl ring may be beneficial for the activity. The binding mode from the docking study consistently predicted that the introduced phenyl ring of 29 can form a  $\pi$ - $\pi$  stack interaction with Tyr191 and Phe133 in an appropriate manner close to the solvent area (Figure 4A). A substituted 1,2,3-triazole was also introduced at this position, resulting in compound 33 with about a threefold improvement in activity. However, introducing pyrimidine and furan groups (31 and 32, respectively) diminished the potency ( $IC_{50}$  = 5.71 and 11.43  $\mu$ M, respectively).

According to the SAR information above, further modifications to the side chain of the phenyl ring were performed to optimize the binding activity and physicochemical properties, resulting in analogues 34–48 (Figure 4B). As shown in Table 4, the binding affinity to WDR5 was significantly improved in all cases except for aromatic substitution (38), with  $IC_{50}$  values ranging from 0.110 to 0.490  $\mu$ M. These compounds maintained their potencies when the amide bond at the 4-position was reversed (34 vs 42 and 35 vs 45). Additionally, the terminal hydrophilic tag may be more beneficial for inhibitory activity (36 vs 46 and 47). Finally, the potency seemed to increase as the length of the linker between the terminal group and the amide increased (39 < 40 < 41, 43 < 44 and 45). As expected, the side chains extended into the solvent area, which is consistent with the prediction (Figure S2).

**SAR of the Core Phenyl Ring.** Since the exact binding mode of this chemotype with WDR5 was not available, we further tried to investigate the substituents on the core phenyl ring. First, based on the previously obtained SAR, a small electron-withdrawing F atom was added to the 6-position of the core phenyl ring; this series of compounds (49–56) resulted in slightly increased inhibitory activities compared to that of compounds without the F substituent (Table 5), indicating a tolerable modification when employing a small substituent. However, introducing an electron-donating methyl group at this position led to the great loss in activity, as seen in 57 ( $IC_{50}$  = 670 nM). Encouragingly, moving the F atom to the 4-position of the core phenyl ring, significantly enhanced the activity, as seen in 58–63. Moreover, compound 64 demonstrated that an electron-donating group was also not suitable at this site. The SARs of the substituents on the upper benzene ring were consistent with that described before. To

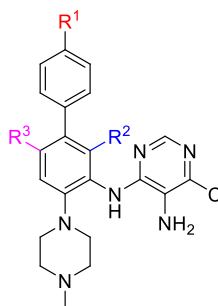
**Table 4. Effects of Side-Chain Phenyl Ring Modifications on WDR5–MLL1 Inhibition**



Compd.	R <sup>1</sup>	FP IC <sub>50</sub> ( $\mu$ M) <sup>a</sup>
34		0.490 ± 0.010
35		0.290 ± 0.020
36		0.370 ± 0.040
37		0.260 ± 0.010
38		5.55 ± 0.020
39		0.190 ± 0.010
40		0.180 ± 0.020
41		0.160 ± 0.010
42		0.420 ± 0.030
43		0.360 ± 0.010
44		0.220 ± 0.010
45		0.230 ± 0.020
46		0.110 ± 0.010
47		0.160 ± 0.010
48		0.460 ± 0.050

<sup>a</sup>IC<sub>50</sub> values represent the mean ± SD of three independent experiments.

Table 5. Effects of the Core Phenyl Ring Substituents on WDR5–MLL1 Inhibition



Compd.	R <sup>1</sup>	R <sup>2</sup>	R <sup>3</sup>	FP IC <sub>50</sub> (nM) <sup>a</sup>
49		-F	-H	240 ± 20
50		-F	-H	117 ± 7.0
51		-F	-H	102 ± 8.0
52		-F	-H	69.0 ± 2.0
53		-F	-H	112 ± 3.0
54		-F	-H	176 ± 1.0
55		-F	-H	105 ± 6.0
56		-F	-H	85.0 ± 5.0
57		-CH <sub>3</sub>	-H	670 ± 10
58		-H	-F	36.0 ± 1.0
59		-H	-F	74.0 ± 3.0
60		-H	-F	21.0 ± 1.0
61		-H	-F	33.0 ± 2.0
62		-H	-F	36.0 ± 1.0
63		-H	-F	29.0 ± 1.0
64		-H	-CH <sub>3</sub>	465 ± 20

<sup>a</sup>IC<sub>50</sub> values represent the mean ± SD of three independent experiments.

understand the reason why a minor change in the structure led to such a great increase in the potency, we compared the docked pose of **52** (Figure 5A) to that of the more active **60** (Figure 5B) in the WDR5 binding site. In contrast to **52**, the F

atom of **60** was capable of forming an additional potential hydrogen bond with the sulfhydryl of Cys261. The result may explain the ca. fourfold improvement of the *in vitro* binding affinity of **60** compared to that of **52**. Together, all these



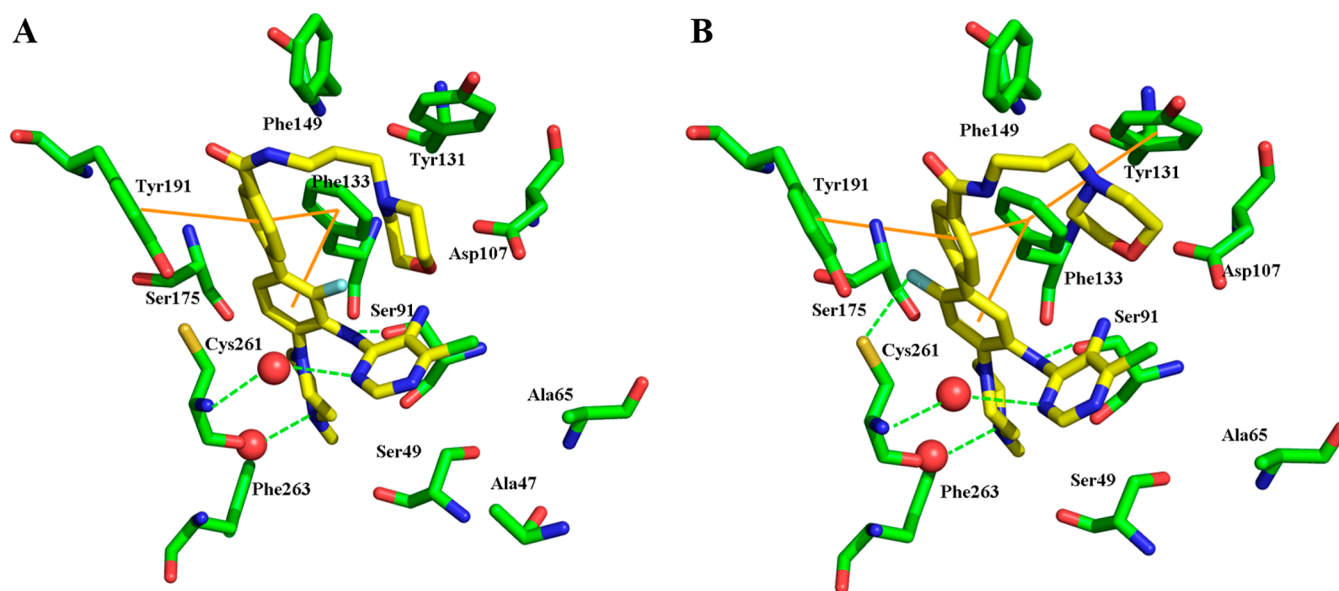


**Figure 5.** Proposed binding modes showing the structures of (A) **52** and (B) **60** docked into WDR5 (PDB 4QL1). Carbons are represented in yellow, the green dashed lines represent the hydrogen bonds, and the orange lines represent the  $\pi$ - $\pi$  stacking interactions.

**Table 6.** Inhibition of Cell Growth and Physicochemical Properties of Representative Compounds

compound	antiproliferation activity IC <sub>50</sub> ( $\mu$ M) <sup>a</sup>				CLogP	$P_e$ at pH 7.4 ( $\times 10^{-6}$ cm/s) <sup>b</sup>
	MV4-11	MOLM-13	K562	HUVEC		
<b>58</b>	19.6 $\pm$ 2.10	16.5 $\pm$ 2.05	88.7 $\pm$ 9.80	>100	3.16	13.73 $\pm$ 0.87
<b>59</b>	27.7 $\pm$ 2.80	23.1 $\pm$ 3.47	>100	>100	3.53	10.51 $\pm$ 0.46
<b>60</b>	25.6 $\pm$ 2.98	17.3 $\pm$ 1.56	70.1 $\pm$ 7.40	>100	3.95	9.140 $\pm$ 0.58
<b>62</b>	15.7 $\pm$ 2.27	12.3 $\pm$ 1.09	81.7 $\pm$ 8.90	>100	4.39	16.87 $\pm$ 0.64
<b>63</b>	12.6 $\pm$ 1.91	13.1 $\pm$ 1.31	>100	>100	3.42	20.22 $\pm$ 1.43

<sup>a</sup>IC<sub>50</sub> values represent the mean  $\pm$  SD of three independent experiments. <sup>b</sup> $P_e$  at pH 7.4 values represent the mean  $\pm$  SD of three independent experiments.

modifications led to a new series of compounds with a  $\sim$ 350-fold improvement on the *in vitro* binding affinity compared to that of hit **9**, such as compound **60** with an IC<sub>50</sub> value of 21.0 nM.

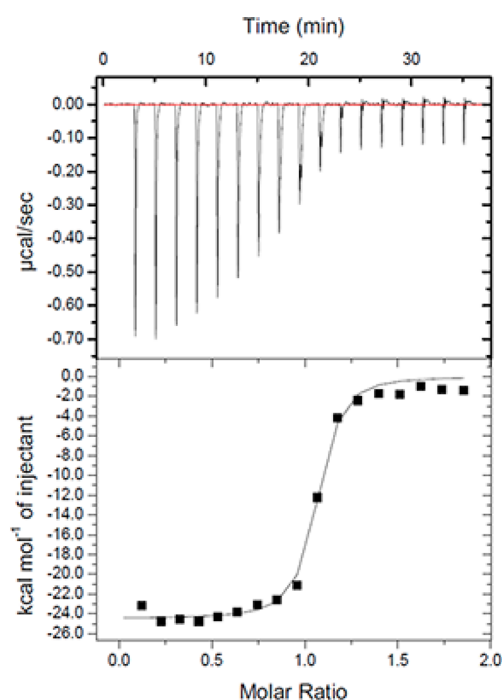
**Antiproliferative Activities and Physicochemical Properties of Representative Compounds.** On the basis of the binding assays, representative compounds were next evaluated for their antiproliferation activity against three human acute leukemia cell lines, including cell lines harboring MLL fusion proteins (MLL-FP, MV4-11, and MOLM-13), a cell line without the MLL fusion protein (K562), and a noncancer cell line (HUVEC, normal human umbilical vein endothelial cells). The data are summarized in Table 6. All compounds showed moderate potencies in terms of inhibiting cell growth in the cell lines harboring MLL fusion proteins. However, these compounds were much less active in the case of the K562 cell line lacking the MLL translocation, showing desirable selectivities between the leukemia cell lines with MLL-FPs and the cell line without MLL-FPs. In addition, these compounds displayed low toxicities against HUVECs, with IC<sub>50</sub> values >100  $\mu$ M indicating their low toxicities against normal cells.

To evaluate the drug-like properties of these analogues, lipid–water distribution coefficients (CLogP) were computationally calculated using the ADMET Predictor 10.0 software. The permeability coefficients ( $P_e$ ) were determined by a standard parallel artificial membrane permeability assay

(PAMPA) on a PAMPA Explore instrument (pION). As shown in Table 6, all compounds showed reasonable lipid–water distribution coefficients. In particular, compound **63** showed the best permeability at pH 7.4. These results may explain, to some degree, why compound **63** displayed the best antiproliferative activity.

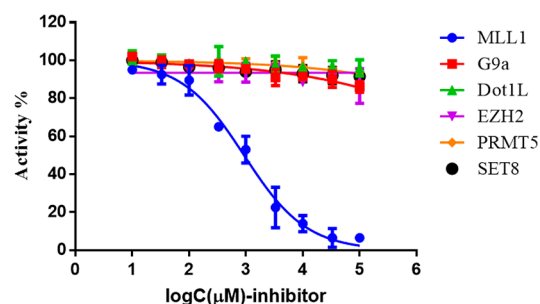
**Biophysical Characterization of Compound 63 Binding to WDR5.** Compound **63** showed impressive inhibitory activity in terms of the WDR5–MLL1 PPI, selective cellular activity toward cell lines harboring MLL fusion proteins, and favorable physicochemical properties. To validate the strong WDR5 binding affinity and analyze the WDR5 binding characteristics of **63**, an isothermal titration calorimetry assay was applied to assess the thermodynamics and affinity of the ligand. The resulting ITC profile gave  $K_d = 72.99$  nM (Figure 6). Notably, the thermodynamic analysis showed that the binding of **63** had a strong enthalpic component ( $\Delta H = -12.25 \pm 0.17$  kcal/mol) and an acceptable entropy ( $T\Delta S = -2.51$  kcal/mol), which suggested that the binding of **63** to WDR5 was an enthalpy-driven process. This binding assay confirmed the direct and tight binding of **63** to the WDR5 protein.

**Compound 63 Selectively Inhibited MLL Complex HMT Activity *In Vitro*.** As mentioned before, the WDR5–MLL1 PPI plays a critical role in the integrity and HMT activity of the MLL1 complex. The assessment of the methylation-inhibitory activity of H3K4 served as a method



$N$	$K_d$ (nM)	$\Delta H$ (kcal · mol <sup>-1</sup> )	$-T\Delta S$ (kcal · mol <sup>-1</sup> )	$\Delta G$ (kcal · mol <sup>-1</sup> )
$1.02 \pm 0.01$	72.99	$-12.25 \pm 0.17$	2.51	-9.73

**Figure 6.** ITC profile of the titration of WDR5 with 63. The thermodynamic parameters of the interaction of WDR5 with 63 as determined by the ITC assay are listed in the table.  $N$  is the stoichiometric coefficient;  $K_d$  is the binding constant;  $\Delta H$ ,  $\Delta S$ , and  $\Delta G$  refer to the changes in binding enthalpy, entropy, and total Gibbs free energy, respectively; and  $\Delta G$  was calculated according to the equation  $\Delta G = \Delta H - T\Delta S$ , where  $T$  is the absolute temperature used for the ITC experiment.



	MLL1 (H3K4)	G9a (H3K9)	DOT1L (H3K79)	EZH2 (H3K27)	SET8 (H4K20)	PRMT5 (H3R8/H4R3)
$IC_{50}(\mu M)$	$0.78 \pm 0.1$	>100	>100	>100	>100	>100

**Figure 7.** Selectivity of compound 63 to the HMT activity of the reconstituted MLL1 core complex over other methyltransferases *in vitro*.

to evaluate the effects on MLL-mediated HMT activity. We therefore evaluated MLL1 HMT activity *in vitro*. Compound 63 efficiently inhibited MLL-mediated HMT activity ( $IC_{50} = 0.78 \mu M$ ) (Figure 7). In addition to the MLL1 complex, 63 was assessed for its inhibitory activity against other protein lysine methyltransferases, including G9a (a H3K9 PKMT), DOT1L (a H3K79 PKMT), EZH2 (a H3K27 PKMT), SET8 (a H4K20 PKMT), and PRMT5 (a protein arginine methyltransferase), and was found to be inactive in these assays ( $IC_{50} > 100 \mu M$ ) (Figure 7). These results indicated

that 63 could selectively inhibit the H3K4 methyltransferase activity of MLL1 *in vitro*.

**Compound 63 Effectively Inhibited MLL Complex HMT Activity and Reduced Downstream Gene Expression in MV4-11 cells.** Based on the inhibition of MLL1 enzymatic activity *in vitro*, the methyltransferase activity of compound 63 in cells was then examined. MV4-11 cells were treated with different concentrations (1, 2.5, 5, and 10  $\mu M$ ) of compounds. As shown in Figure 8A, compound 63 induced the concentration-dependent downregulation of

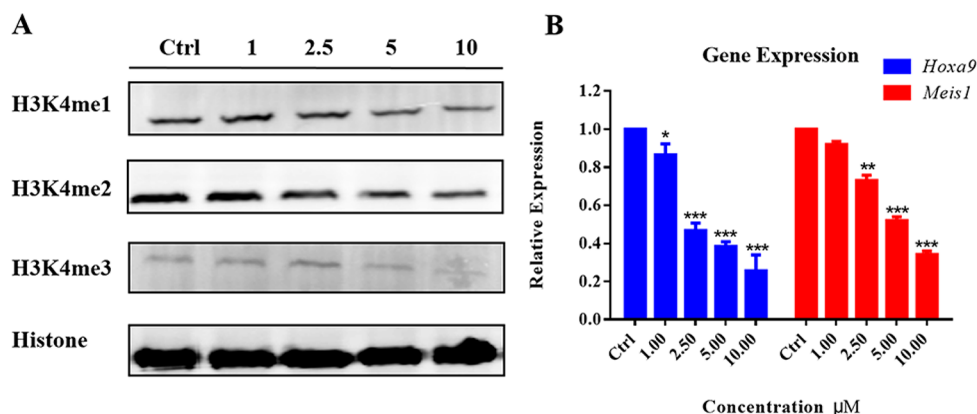


**Figure 8.** (A) Western blot analyses for H3K4 methylation activity after the treatment of MV4-11 cells with DMSO and 1, 2.5, 5.0, and 10  $\mu$ M compound 63 for seven days. H3K4me1, H3K4me2, and H3K4me3 were determined using histone as loading control. (B) The inhibition of *Hoxa9* and *Meis1* gene expressions after treatment with different concentrations (0, 1, 2.5, 5, and 10  $\mu$ M) of compound 63 in MV4-11 cells for seven days as assessed by RT-PCR. Each experiment was performed in triplicate ( $n = 3$ ). \* $p < 0.05$ , \*\* $p < 0.01$ , and \*\*\* $p < 0.001$  as calculated by Student's  $t$ -tests.

H3K4me1, H3K4me2, and H3K4me3, showing the inhibition of the methyltransferase activity of MLL1 in cells.

MLL1 is essential for development, neurogenesis, and hematopoiesis through the regulation of *Hox* genes and the expression of other transcription cofactors.<sup>41–45</sup> The dysregulation of *Hox* genes and the cofactor *Meis1* gene was observed in leukemias associated with MLL1 genetic rearrangements.<sup>46</sup> Thus, we investigated the effects of 63 on the MLL1 downstream gene expression in MV4-11 cells. As shown in Figure 8B, compound 63 decreased the mRNA level of *Hoxa9* and *Meis1* in MV4-11 cells in a concentration-dependant manner. This result indicated that disturbing the WDR5–MLL1 PPI with 63 efficiently regulated the expression of MLL1 fusion protein-dependent genes.

**Metabolic and Pharmacokinetic Profiles of 63.** We further examined the metabolic stability of 63 *in vitro* in human and rat liver microsomes. As shown in Table 7, compound 63 possessed a suitable metabolic stability, with half-life values >60 min in both human and rat liver microsomes.

**Table 7. *In Vitro* Metabolic Stability in Human and Rat Liver Microsomes of 63**

compound	human liver microsomes		rat liver microsomes	
	$T_{1/2}$ (min)	CL ( $\mu$ L/min/mg)	$T_{1/2}$ (min)	CL ( $\mu$ L/min/mg)
63	70.0	14.1	66.0	15.0

With the aim to explore the potentially use of 63 in acute leukemia models *in vivo* and determine the method of administration, we next undertook an assessment of pharmacokinetic (PK) parameters in healthy rats (Table 8). 63 exhibited an acceptable half-life ( $T_{1/2}$ ) ( $4.94 \pm 0.04$  h) after oral administration. Moreover, a good bioavailability was observed ( $F = 82.1\%$ ), verifying the oral administration of this compound for further research *in vivo*.

***In Vivo* Antitumor Efficacy of 63.** With the potent inhibitory activity and drug-like properties both *in vitro* and *in vivo* established, compound 63 was further assessed in an MV4-11 xenograft model to examine its *in vivo* antitumor efficacy. In this study, the hydrochloride salt of compound 63 was administered daily to mice by oral administration at 40, 80, and 120 mg/kg for three weeks. As shown in Figure 9,

**Table 8. *In Vivo* Pharmacokinetic Profiles<sup>a</sup> of 63**

parameters	<i>p.o.</i> (10 mg/kg)	<i>i.v.</i> (2 mg/kg)
$t_{1/2}$ (hr)	$4.94 \pm 0.04$	$1.70 \pm 0.63$
$t_{max}$ (hr)	$2.00 \pm 1.73$	
$C_{max}$ (ng/mL)	$159 \pm 60.0$	
$AUC_{0-t}$ (ng·hr/mL)	$1316 \pm 683$	$411 \pm 90.6$
$AUC_{0-\infty}$ (ng·hr/mL)	$1738 \pm 255$	$424 \pm 98$
$V_z$ (L/kg)	$37.1 \pm 11.3$	$12.2 \pm 6.24$
$Cl_F$ (mL/min/kg)	$97.2 \pm 14.0$	$81.3 \pm 16.7$
MRT (hr)	$5.42 \pm 1.20$	$1.18 \pm 0.40$
bioavailability (%)	82.1%	

<sup>a</sup> $C_{max}$ , maximum plasma concentration;  $t_{max}$ , time to reach the maximum plasma concentration; AUC, area under the plasma concentration–time curve;  $t_{1/2}$ , half-life; MRT, mean residence time;  $V_z$ , apparent volume of distribution;  $Cl_F$ , apparent clearance;  $n = 3$ , mean  $\pm$  SEM.

compound 63 significantly inhibited the tumor growth. The tumor volume growth inhibition (GI) values of the mice treated with 40, 80, and 120 mg/kg doses of 63 were 39.40%, 53.59%, and 54.51%, respectively (Figure 9A). Simultaneously, treatment at the dosage of 40 mg/kg led to 36.43% tumor weight growth inhibition (TGI) compared with the control (Figure 9B). Nevertheless, the antitumor effects did not increase significantly at doses of 80 and 120 mg/kg, which may need to be further explored. In addition, compound 63 was well tolerated, and no significant loss of body weight was observed in 63-treated mice during the treatment period (Figure 9C). These results suggested that 63 had potential efficacy against the growth of implanted MV4-11 cells in mice.

**Chemistry.** The target compounds 8–28 were synthesized using routes summarized in Scheme 1. Commercially available 2-fluoro-5-nitroaniline 65 was reacted with 1-methyl piperazine to give the intermediate 66, which was then coupled with the corresponding chlorinated heterocyclic to give compounds 8, 19, and 22, respectively. The substitution reaction of 65 with different pyrimidines afforded intermediates 67a–67i, which were then reacted with 1-methyl piperazine to create compounds 9, 13–18, 20, and 21, respectively. The chlorine atom of 9 was substituted with different secondary amines to obtain target compounds 10–12. The fluorine atom of

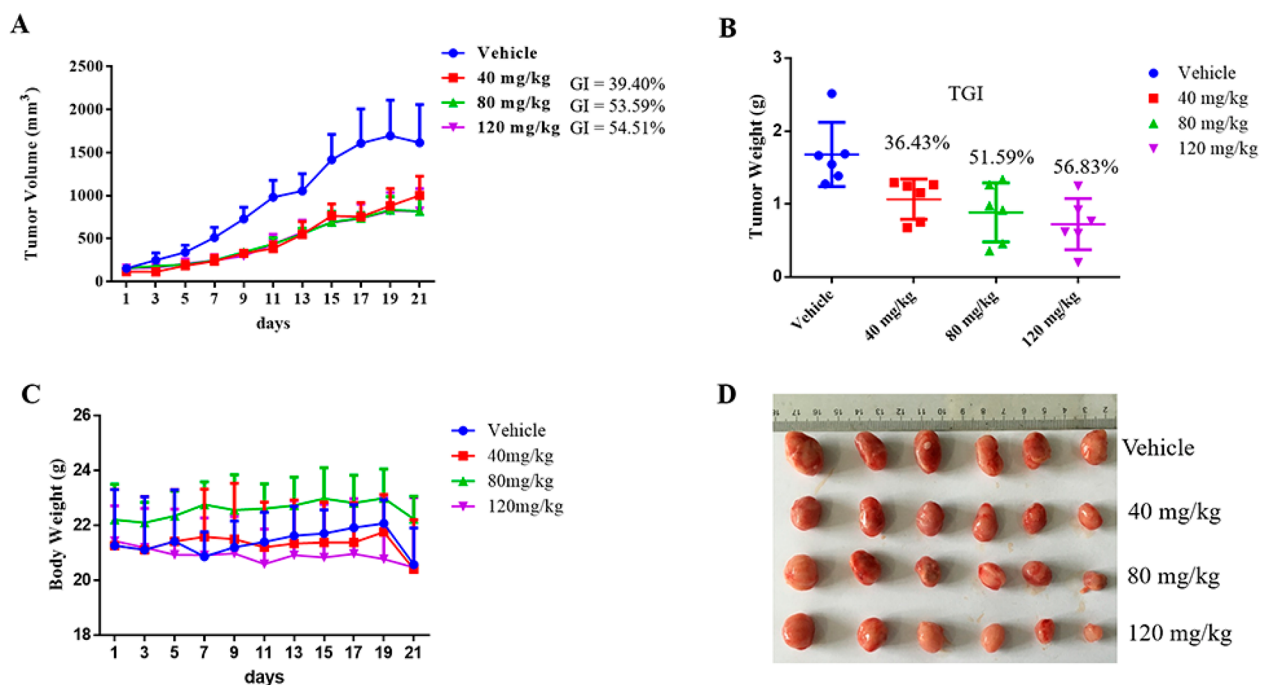
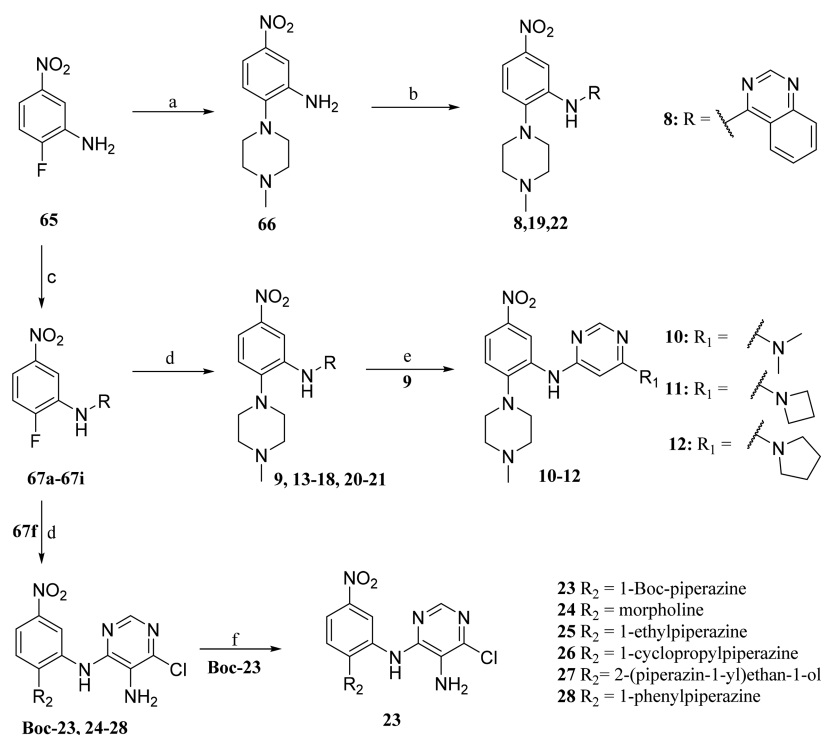


**Figure 9.** Compound 63 suppressed the tumor growth *in vivo* in the MV4-11 tumor xenografts nude model. (A) Changes in the tumor volume of MV4-11 tumor-bearing mice after treatment for three weeks. (B) Tumor weights after treatment. (C) Body weights of the treated mice. (D) Images of the excised tumors for each group.

#### Scheme 1. Synthetic Routes for Compounds 8–28<sup>a</sup>

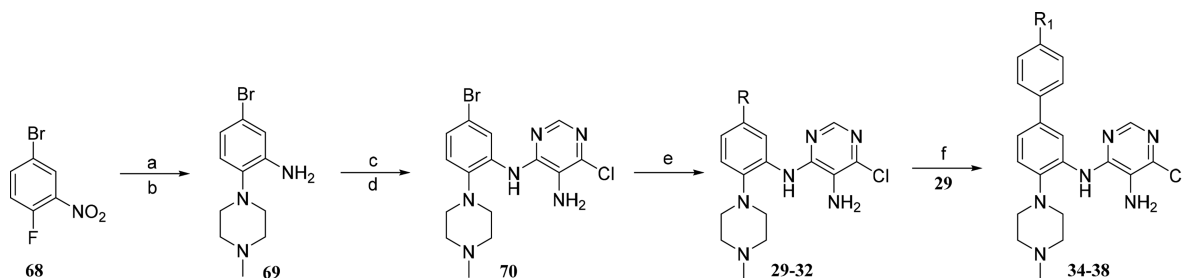


<sup>a</sup>Reagents and conditions are as follows: (a) 1-methyl piperazine, DMF, DIPEA, 100 °C, 8 h, 53%; (b) the corresponding chlorinated heterocyclic, dioxane, Pd<sub>2</sub>(dba)<sub>3</sub>, BINAP, Cs<sub>2</sub>CO<sub>3</sub>, 100 °C, 12 h, 37–64%; (c) pyrimidines, IPA (EtOH/H<sub>2</sub>O), HCl, reflux, 18–24 h, 56–86%; (d) different secondary amines, DMF, DIPEA, 50 °C, 2–5 h, 45–89%; (e) different amines, DMF, DIPEA, 120 °C, 4–6 h, 47–50%; (f) DCM/MeOH, TFA, r.t., 2 h, 65%. The detailed R groups for 9–22 are shown in Table 1.

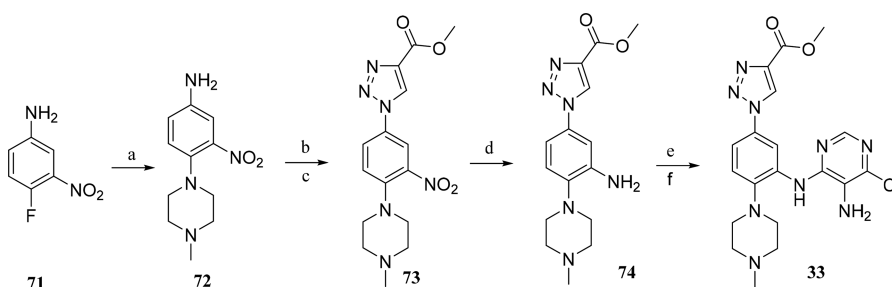
intermediate **67i** was substituted with different piperazines or morpholine to yield the target compounds **23–28**.

The synthesis of compounds **29–32** and **34–38** are shown in Scheme 2. The substitution reaction of **68** with 1-methyl

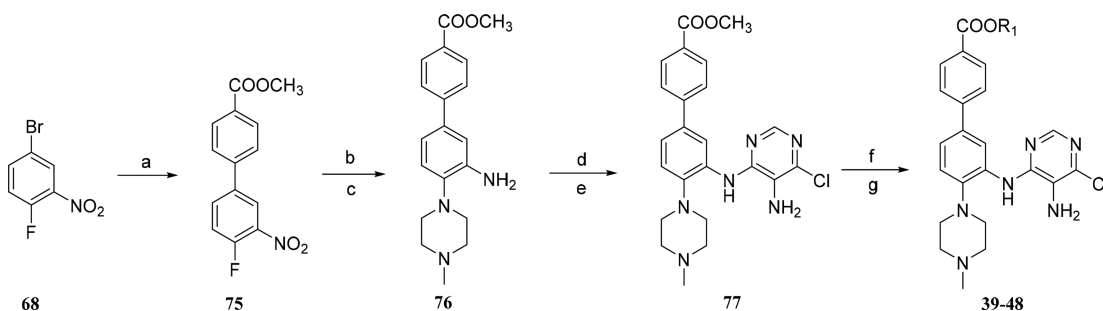
piperazine and the reduction of the nitro group with hydrogen and Pd/C gave **69**. Subsequent substitution and reduction yielded **70**. Then, **70** was reacted with different boronic acids through the Suzuki coupling reaction in the presence of

Scheme 2. Synthetic Routes for the Target Compounds 29–32 and 34–38<sup>a</sup>

<sup>a</sup>Reagents and conditions are as follows: (a) 1-methyl piperazine, DMF, DIPEA, 80 °C, 5 h; (b) Pd/C, H<sub>2</sub>, r.t., 2 h, 86%; (c) 4,6-dichloro-5-nitropyrimidine, THF, Et<sub>3</sub>N, 0 °C, 6 h; (d) SnCl<sub>2</sub>, EA, reflux, 4 h, 75%; (e) different boronic acids, Pd(PPh<sub>3</sub>)<sub>2</sub>Cl<sub>2</sub>, Cs<sub>2</sub>CO<sub>3</sub>, dioxane, reflux, 20 h, 46–70%; (f) acids, BOP, Et<sub>3</sub>N, DMF, r.t., 12 h, 64–80%. The detailed R groups for 29–32 are shown in Table 3, and R<sub>1</sub> groups for 34–38 are shown in Table 4.

Scheme 3. Synthetic Routes for the Target Compound 33<sup>a</sup>

<sup>a</sup>Reagents and conditions are as follows: (a) 1-methylpiperazine, DIPEA, CH<sub>3</sub>CN, reflux, 12 h, 95%; (b) (i) NaNO<sub>2</sub>, 6 M/HCl, 0 °C, 0.5 h, (ii) NaN<sub>3</sub>, 0 °C, 0.5 h, then r.t., 2 h; (c) methyl propiolate, CuI, MeOH, DIPEA, reflux, 48 h, 63%; (d) H<sub>2</sub>, Pd/C, MeOH, r.t., 6 h, 85%; (e) 4,6-dichloro-5-nitropyrimidine, THF, Et<sub>3</sub>N, 0 °C, 6 h; (f) SnCl<sub>2</sub>, EA, reflux, 4 h, 66%.

Scheme 4. Synthetic Routes for the Target Compounds 39–48<sup>a</sup>

<sup>a</sup>Reagents and conditions are as follows: (a) (4-(methoxycarbonyl)phenyl)boronic acid, Pd(PPh<sub>3</sub>)<sub>2</sub>Cl<sub>2</sub>, Cs<sub>2</sub>CO<sub>3</sub>, dioxane, reflux, 20 h, 70%; (b) 1-methylpiperazine, CH<sub>3</sub>CN, DIPEA, 80 °C, 5 h; (c) Pd/C, H<sub>2</sub>, r.t., 2 h, 85%; (d) 4,6-dichloro-5-nitropyrimidine, THF, Et<sub>3</sub>N, 0 °C, 2–6 h; (e) SnCl<sub>2</sub>, EA, reflux, 4 h, 46%; (f) 1 M LiOH, MeOH, r.t., 2 h; (g) different amines, BOP, Et<sub>3</sub>N, DMF, r.t., 12 h, 42–79%. The detailed R groups for 39–48 are shown in Table 4.

Cs<sub>2</sub>CO<sub>3</sub> to obtain 29–32. Compound 29 was condensed with corresponding acids to afford compounds 34–38.

The synthetic route of compound 33 is listed in Scheme 3. Briefly, 4-fluoro-3-nitroaniline 71 was substituted with *N*-methylpiperazine to produce intermediate 72. The key intermediate 73 was prepared by diazotization to form the azide and cyclized via click chemistry. Subsequent reduction, substitution, and reduction reactions yielded the target compound 33.

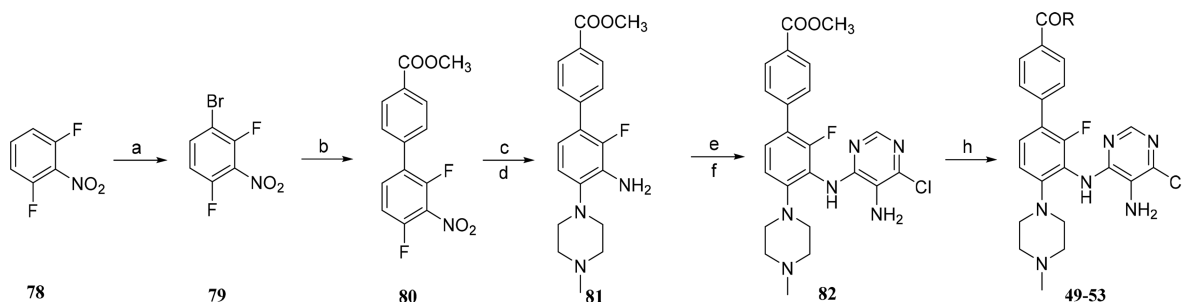
The compounds 39–48 were synthesized according to Scheme 4. 68 was reacted with (4-(methoxycarbonyl)phenyl)-boronic acid via coupling to create the intermediate 75. 76 was synthesized similar to 69. After similar substitution and reduction reactions, 77 was obtained. Then, the ester group

was hydrolyzed by LiOH in MeOH/H<sub>2</sub>O, and the subsequent condensation with different amines generated compounds 39–48.

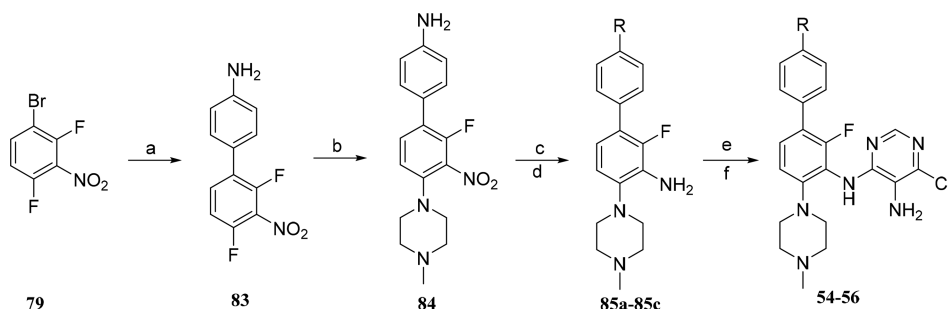
The compounds 49–53 were synthesized (Scheme 5) from commercially available 2,6-difluoronitrobenzene. 79 was obtained by an NBS bromination reaction, and the target compounds 49–53 were synthesized similar to 39.

The synthesis of compounds 54–56 are shown in Scheme 6. The intermediate 84 was obtained by coupling and substitution reactions from 79. To avoid the selective condensation of amino groups, 84 was first acylated with different acids, then nitro groups of the core phenyl were reduced to afford 85a–85c. Subsequently, analogues 54–56,

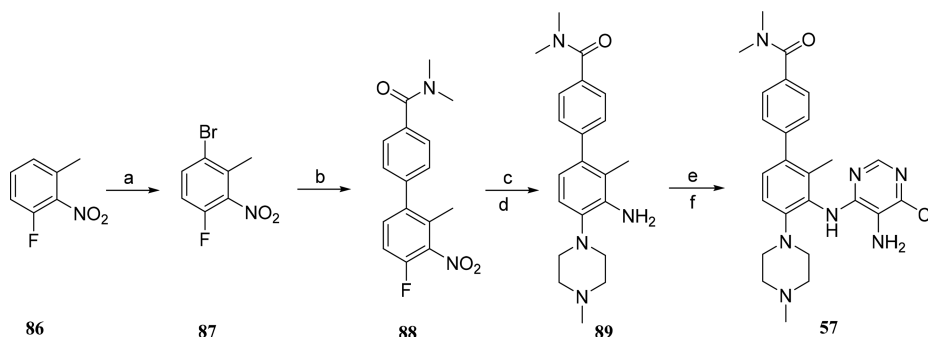


Scheme 5. Synthetic Routes for the Target Compounds 49–53<sup>a</sup>

<sup>a</sup>Reagents and conditions are as follows: (a) NBS, TFA, H<sub>2</sub>SO<sub>4</sub>, 0 °C, 18 h, 90%; (b) (4-(methoxycarbonyl)phenyl)boronic acid, Pd(PPh<sub>3</sub>)<sub>2</sub>Cl<sub>2</sub>, Cs<sub>2</sub>CO<sub>3</sub>, dioxane, reflux, 20 h, 65%; (c) 1-methyl piperazine, DMF, DIPEA, 80 °C, 5 h; (d) Pd/C, H<sub>2</sub>, r.t., 2 h, 65%; (e) 4,6-dichloro-5-nitropyrimidine, THF, Et<sub>3</sub>N, 0 °C, 6 h; (f) SnCl<sub>2</sub>, EA, reflux, 4 h, 56%; (g) 1 M LiOH, MeOH, r.t., 2 h; (h) different amines, BOP, Et<sub>3</sub>N, DMF, r.t., 12 h. The detailed R groups for 49–53 are shown in Table 5.

Scheme 6. Synthetic Routes for the Target Compounds 54–56<sup>a</sup>

<sup>a</sup>Reagents and conditions are as follows: (a) (4-aminophenyl)boronic acid, Pd(PPh<sub>3</sub>)<sub>2</sub>Cl<sub>2</sub>, Cs<sub>2</sub>CO<sub>3</sub>, dioxane, reflux, 20 h, 69%; (b) 1-methylpiperazine, CH<sub>3</sub>CN, DIPEA, 80 °C, 5 h, 88%; (c) different acids, HATU, Et<sub>3</sub>N, DMF, r.t., 12 h; (d) Pd/C, H<sub>2</sub>, r.t., 2 h, 69–88%; (e) 4,6-dichloro-5-nitropyrimidine, THF, Et<sub>3</sub>N, 0 °C, 2–6 h; (f) SnCl<sub>2</sub>, EA, reflux, 4 h, 35–38%.

Scheme 7. Synthetic Routes for the Target Compound 57<sup>a</sup>

<sup>a</sup>Reagents and conditions are as follows: (a) NBS, TFA, H<sub>2</sub>SO<sub>4</sub>, 0 °C, 18 h, 87%; (b) (4-(dimethylcarbamoyl)phenyl)boronic acid, Pd(PPh<sub>3</sub>)<sub>2</sub>Cl<sub>2</sub>, Cs<sub>2</sub>CO<sub>3</sub>, dioxane, reflux, 20 h, 77%; (c) 1-methylpiperazine, CH<sub>3</sub>CN, DIPEA, 80 °C, 5 h; (d) Pd/C, H<sub>2</sub>, r.t., 2 h, 65%; (e) 4,6-dichloro-5-nitropyrimidine, THF, Et<sub>3</sub>N, 0 °C, 6 h; (f) SnCl<sub>2</sub>, EA, reflux, 4 h, 44%.

respectively, were synthesized according to a procedure similar to that of 33.

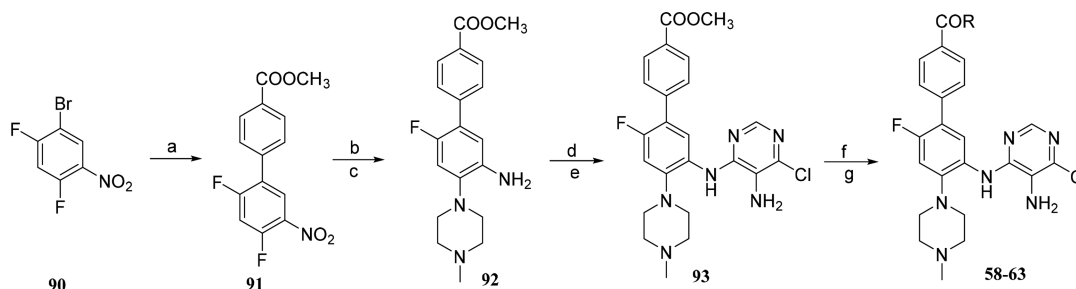
The compound 57 was synthesized (Scheme 7) from commercially available 2-fluoro-6-methyl nitrobenzene. 87 was obtained by an NBS bromination reaction, then the target compound 57 was synthesized similar to 54.

The synthesis of compounds 58–63 are shown in Scheme 8. Analogues 58–63 were synthesized from commercially available 1-bromo-2,4-difluoro-5-nitrobenzene according to a procedure similar to that of 49.

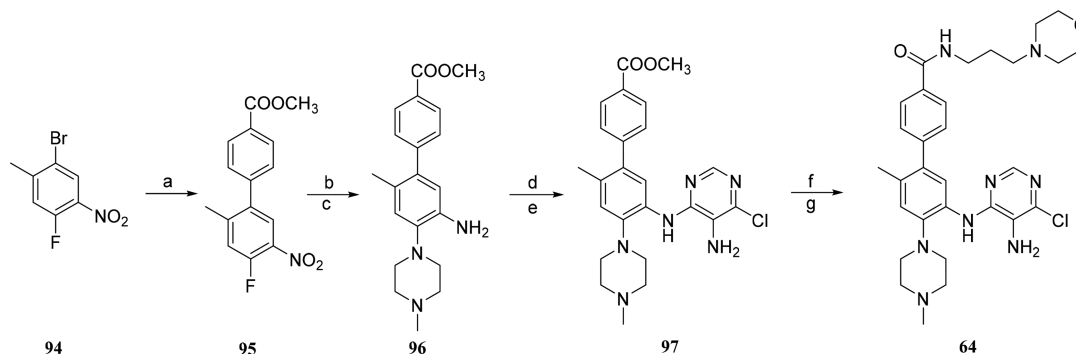
Compound 64 was synthesized (Scheme 9) starting from commercially available 2-fluoro-6-methyl nitrobenzene according to a procedure similar to that of 60.

## CONCLUSIONS

The dysregulation of MLL1 catalytic functions is associated with MLL-rearranged cancers. Directly disrupting the WDR5–MLL1 PPI has been increasingly recognized as a target and a specific way to develop potential therapeutic agents. However, the efficacy of small-molecule WDR5–MLL1 inhibitors *in vivo* is still unclear. In this study, we initially identified compound 9 as an active hit with an aniline pyrimidine scaffold by utilizing a

Scheme 8. Synthetic Routes for the Target Compounds 58–63<sup>a</sup>

<sup>a</sup>Reagents and conditions are as follows: (a) (4-(methoxycarbonyl)phenyl)boronic acid, Pd(PPh<sub>3</sub>)<sub>2</sub>Cl<sub>2</sub>, Cs<sub>2</sub>CO<sub>3</sub>, dioxane, reflux, 20 h, 68%; (b) 1-methylpiperazine, CH<sub>3</sub>CN, DIPEA, 80 °C, 5 h; (c) Pd/C, H<sub>2</sub>, r.t., 2 h, 64%; (d) 4,6-dichloro-5-nitropyrimidine, THF, Et<sub>3</sub>N, 0 °C, 6 h; (e) SnCl<sub>2</sub>, EA, reflux, 4 h, 57%; (f) 1 M LiOH, MeOH, r.t., 2 h; (g) different amines, BOP, Et<sub>3</sub>N, DMF, r.t., 12 h, 65–78%.

Scheme 9. Synthetic Routes for the Target Compound 64<sup>a</sup>

<sup>a</sup>Reagents and conditions are as follows: (a) (4-(methoxycarbonyl)phenyl)boronic acid, Pd(PPh<sub>3</sub>)<sub>2</sub>Cl<sub>2</sub>, Cs<sub>2</sub>CO<sub>3</sub>, dioxane, reflux, 20 h, 69%; (b) 1-methylpiperazine, CH<sub>3</sub>CN, DIPEA, 80 °C, 5 h; (c) Pd/C, H<sub>2</sub>, r.t., 2 h, 65%; (d) 4,6-dichloro-5-nitropyrimidine, THF, Et<sub>3</sub>N, 0 °C, 6 h; (e) SnCl<sub>2</sub>, EA, reflux, 4 h, 46%; (f) 1 M LiOH, MeOH, r.t., 2 h; (g) different amines, BOP, Et<sub>3</sub>N, DMF, r.t., 12 h, 78%.

scaffold-hopping strategy from benzamide inhibitor **3**. Then, further systematic SAR studies led to the discovery of inhibitor **63**, which has the most efficient WDR5 inhibitory activity as well as preferable physicochemical properties, making it a valuable asset for further research. Compound **63** showed the selective inhibition of the proliferation of MLL-FPs leukemia cells over K562 cells without MLL-FPs and displayed little toxicity to the noncancerous human cell line. In addition, we described its inhibition activity of the MLL histone methyltransferase *in vitro* and in cells, followed by the validation of the downregulation of MLL fusion protein-dependent genes. Moreover, **63** possessed an ideal metabolic stability in both human and rat microsomes and an appropriate pharmacokinetic profile for oral administration. Additionally, **63** demonstrated potent *in vivo* activity in MV4-11 xenograft tumors in mice. In conclusion, we discovered a new chemotype small-molecule inhibitor of WDR5–MLL1 PPI that served as a potential starting point toward MLL1-driven acute myeloid leukemia carrying MLL translocation therapeutics. We hope these results can provide useful implications for the development of therapeutic agents to target WDR5–MLL1.

## EXPERIMENTAL SECTION

**General Chemistry.** The synthesis of the test compounds is highlighted in Schemes 1–9. All reagents were purchased from commercial sources. Organic solvents were concentrated via an evaporator (Büchi Rotavapor) below 60 °C under reduced pressure. Melting points (mp) were detected by a Melt-Temp II apparatus. All the reactions were monitored

using TLC silica gel plates (GF254, 0.25 mm) and visualized under UV light. The <sup>1</sup>H NMR and <sup>13</sup>C NMR spectra were recorded on a Bruker AV-300 instrument using deuterated solvents with tetramethylsilane (TMS) as internal standard. EI-MS were recorded on Shimadzu Model GCMS-2010 instruments. ESI-MS and high-resolution mass spectra (HRMS) were collected on a Waters Q-ToF micro mass spectrometer (all data were within 0.40% of the theoretical values). The purity (≥95%) of the target compounds was verified by high-performance liquid chromatography (HPLC) analysis (Agilent C18 column, 4.6 mm × 150 mm, 0.5 mL/min).

**N-(2-(4-Methylpiperazin-1-yl)-5-nitrophenyl)quinazolin-4-amine (8).** **66** (0.2 g, 0.846 mmol) was dissolved in the solution of 1,4-dioxane (20 mL), Pd<sub>2</sub>(dba)<sub>3</sub> (0.15 g, 0.253 mmol), and BINAP (0.12 g, 0.13 mmol). Then, 4-chloroquinazoline (0.27 g, 1.69 mmol) and Cs<sub>2</sub>CO<sub>3</sub> were added into the mixture. The reaction was carried out in 100 °C for 12 h under the protection of nitrogen. After cooling to the room temperature, the reaction mixture was filtered to remove the catalytic agent and Cs<sub>2</sub>CO<sub>3</sub>. Then, the solvent was removed by a rotary evaporator and purified by column chromatography on silica gel to afford compound **8** as light yellow solid. Yield: 63%. mp >250 °C. <sup>1</sup>H NMR (300 MHz, DMSO-*d*<sub>6</sub>): δ 9.57 (s, 1H), 8.61 (s, 2H), 8.43 (s, 1H), 8.07 (s, 1H), 7.86 (d, *J* = 10.0 Hz, 2H), 7.69 (s, 1H), 7.30 (s, *J* = 8.8 Hz, 1H), 3.09 (s, 4H), 2.32 (s, 4H), 2.13 (s, 3H). HRMS (ESI): calcd. for *m/z* C<sub>19</sub>H<sub>20</sub>N<sub>6</sub>O<sub>2</sub>, [M + H]<sup>+</sup> 365.1720, found 365.1722. HPLC (100% MeOH): *t*<sub>R</sub> = 7.772 min, 99.16%.

*N*<sup>4</sup>-(2-(4-Methylpiperazin-1-yl)-5-nitrophenyl)pyrimidine-4,5-diamine (**19**). The same procedure as **8**. Yellow solid, yield: 44%. mp >250 °C. <sup>1</sup>H NMR (300 MHz, DMSO-*d*<sub>6</sub>): δ 8.25 (s, 1H), 7.82 (dd, *J* = 7.4, 1.9 Hz, 1H), 7.81–7.77 (m, 2H), 7.67 (s, 1H), 7.04 (d, *J* = 7.5 Hz, 1H), 5.82 (s, 2H), 3.20 (t, *J* = 5.3 Hz, 4H), 2.98 (t, *J* = 5.3 Hz, 4H), 2.60 (s, 3H). HRMS (ESI): calcd. for *m/z* C<sub>15</sub>H<sub>19</sub>N<sub>7</sub>O<sub>2</sub>, [M + H]<sup>+</sup> 330.1673, found 330.1675. HPLC (100% MeOH): *t*<sub>R</sub> = 7.673 min, 97.05%.

*N*<sup>2</sup>-(2-(4-Methylpiperazin-1-yl)-5-nitrophenyl)pyridine-2,3-diamine (**22**). The same procedure as **8**. Yellow solid, yield: 37%. mp 210–212 °C. <sup>1</sup>H NMR (300 MHz, DMSO-*d*<sub>6</sub>): δ 9.06 (d, *J* = 2.8 Hz, 1H), 7.77 (dd, *J* = 8.8, 2.8 Hz, 1H), 7.68–7.59 (m, 2H), 7.28 (d, *J* = 8.8 Hz, 1H), 7.77 (dd, *J* = 7.6, 1.7 Hz, 1H), 6.75 (dd, *J* = 7.6, 1.7 Hz, 1H), 4.94 (s, 2H), 2.90 (t, *J* = 4.8 Hz, 4H), 2.54 (s, 4H), 2.25 (s, 3H). HRMS (ESI): calcd. for *m/z* C<sub>15</sub>H<sub>20</sub>N<sub>6</sub>O<sub>2</sub>, [M + H]<sup>+</sup> 329.1720, found 329.1722. HPLC (100% MeOH): *t*<sub>R</sub> = 4.151 min, 95.29%.

**General Procedure for the Synthesis of the Compounds 9, 13–18, and 20–21.** The intermediates **67a–67i** (1 mmol) were dissolved in the solution of DMF (5 mL) and DIPEA (3 mmol) before the addition of 1-methyl piperazine (3 mmol). The reaction was carried out at 50 °C for 2–5 h. The reaction mixture was subsequently diluted with dichloromethane (20 mL) and washed with water (3 × 10 mL) and a saturated sodium chloride solution (10 mL). The organic phase was then separated, dried with sodium sulfate (Na<sub>2</sub>SO<sub>4</sub>), filtered, and concentrated to provide crude products. The crude products were washed with CH<sub>3</sub>CN (5 mL) to obtain **9**, **13–18**, **20**, and **21** as yellow solids.

6-Chloro-*N*-(2-(4-methylpiperazin-1-yl)-5-nitrophenyl)pyrimidin-4-amine (**9**). Yield: 66%. mp 169–171 °C. <sup>1</sup>H NMR (300 MHz, DMSO-*d*<sub>6</sub>): δ 9.36 (s, 1H), 8.48 (s, 1H), 8.42 (d, *J* = 2.7 Hz, 1H), 8.02 (dd, *J* = 8.9, 2.8 Hz, 1H), 7.23 (d, *J* = 9.0 Hz, 1H), 6.81 (s, 1H), 3.04 (t, *J* = 4.6 Hz, 4H), 2.35 (t, *J* = 4.7 Hz, 4H), 2.16 (s, 3H). <sup>13</sup>C NMR (75 MHz, DMSO-*d*<sub>6</sub>): δ 161.34, 158.74, 158.69, 151.70, 141.57, 130.46, 129.94, 121.67, 121.11, 119.89, 105.90, 54.60, 49.90, 46.16. HRMS (ESI): calcd. for *m/z* C<sub>15</sub>H<sub>17</sub>ClN<sub>6</sub>O<sub>2</sub>, [M + H]<sup>+</sup> 349.1174, found 349.1177. HPLC (100% MeOH): *t*<sub>R</sub> = 6.097 min, 96.84%.

6-Chloro-2-methyl-*N*-(2-(4-methylpiperazin-1-yl)-5-nitrophenyl)pyrimidin-4-amine (**13**). Yield: 45%. mp 196–198 °C. <sup>1</sup>H NMR (300 MHz, CDCl<sub>3</sub>): δ 9.09 (d, *J* = 2.6 Hz, 1H), 7.97 (dd, *J* = 8.8, 2.7 Hz, 1H), 7.55 (s, 1H), 7.23 (s, 1H), 6.59 (s, 1H), 3.02 (t, *J* = 4.8 Hz, 4H), 2.65–2.61 (m, 7H), 2.40 (s, 3H). HRMS (ESI): calcd. for *m/z* C<sub>16</sub>H<sub>19</sub>ClN<sub>6</sub>O<sub>2</sub>, [M + H]<sup>+</sup> 363.1331, found 363.1335. HPLC (100% MeOH): *t*<sub>R</sub> = 8.574 min, 97.99%.

6-Chloro-*N*<sup>4</sup>-(2-(4-methylpiperazin-1-yl)-5-nitrophenyl)pyrimidine-2,4-diamine (**14**). Yield: 78%. mp 248–251 °C. <sup>1</sup>H NMR (300 MHz, CDCl<sub>3</sub>): δ 9.13 (s, 1H), 7.94 (dd, *J* = 8.7, 2.6 Hz, 1H), 7.41 (s, 1H), 7.20 (d, *J* = 2.6 Hz, 1H), 5.16 (s, 2H), 3.00 (t, *J* = 4.8 Hz, 4H), 2.64 (s, 4H), 2.41 (s, 3H). HRMS (ESI): calcd. for *m/z* C<sub>15</sub>H<sub>18</sub>ClN<sub>7</sub>O<sub>2</sub>, [M + H]<sup>+</sup> 364.1283, found 364.1289. HPLC (100% MeOH): *t*<sub>R</sub> = 5.850 min, 97.14%.

6-Chloro-5-methyl-*N*-(2-(4-methylpiperazin-1-yl)-5-nitrophenyl)pyrimidin-4-amine (**15**). Yield: 60%. mp 259–261 °C. <sup>1</sup>H NMR (300 MHz, CDCl<sub>3</sub>): δ 9.55 (s, 1H), 8.57 (s, 1H), 8.18 (s, 1H), 7.95 (dd, *J* = 8.7, 2.7 Hz, 1H), 7.27 (s, 1H), 3.02 (t, *J* = 4.8 Hz, 4H), 2.66 (s, 4H), 2.42 (s, 6H). HRMS (ESI): calcd. for *m/z* C<sub>16</sub>H<sub>19</sub>ClN<sub>6</sub>O<sub>2</sub>, [M + H]<sup>+</sup> 363.1331,

found 363.1349. HPLC (100% MeOH): *t*<sub>R</sub> = 6.297 min, 95.67%.

6-Chloro-*N*-(2-(4-methylpiperazin-1-yl)-5-nitrophenyl)-5-nitropyrimidin-4-amine (**16**). Yield: 53%. mp >250 °C. <sup>1</sup>H NMR (300 MHz, DMSO-*d*<sub>6</sub>): δ 10.20 (s, 1H), 8.85 (d, *J* = 6.5 Hz, 1H), 8.16 (d, *J* = 6.0 Hz, 2H), 7.62 (t, *J* = 9.5 Hz, 1H), 3.52 (br s, 4H), 2.42 (br s, 4H), 2.22 (s, 3H). HRMS (ESI): calcd. for *m/z* C<sub>15</sub>H<sub>16</sub>ClN<sub>7</sub>O<sub>4</sub>, [M + H]<sup>+</sup> 394.0671, found 394.0674. HPLC (100% MeOH): *t*<sub>R</sub> = 6.083 min, 97.01%.

6-Chloro-*N*<sup>4</sup>-(2-(4-methylpiperazin-1-yl)-5-nitrophenyl)pyrimidine-4,5-diamine (**17**). Yield: 85%. mp 185–187 °C. <sup>1</sup>H NMR (300 MHz, DMSO-*d*<sub>6</sub>): δ 8.65 (d, *J* = 2.6 Hz, 1H), 8.22 (s, 1H), 7.98–7.91 (m, 2H), 7.27 (d, *J* = 8.9 Hz, 1H), 5.41 (s, 2H), 2.91 (br s, 4H), 2.47 (br s, 4H), 2.20 (s, 3H). HRMS (ESI): calcd. for *m/z* C<sub>15</sub>H<sub>18</sub>ClN<sub>7</sub>O<sub>2</sub>, [M + H]<sup>+</sup> 364.1283, found 364.1286. HPLC (100% MeOH): *t*<sub>R</sub> = 6.581 min, 98.22%.

6-Chloro-2-methyl-*N*<sup>4</sup>-(2-(4-methylpiperazin-1-yl)-5-nitrophenyl)pyrimidine-4,5-diamine (**18**). Yield: 68%. mp 248–250 °C. <sup>1</sup>H NMR (300 MHz, DMSO-*d*<sub>6</sub>): δ 8.87 (d, *J* = 2.8 Hz, 1H), 8.22 (s, 1H), 7.94 (dd, *J* = 8.8, 2.8 Hz, 1H), 7.28 (d, *J* = 8.9 Hz, 1H), 5.12 (s, 2H), 2.98 (t, *J* = 4.8 Hz, 4H), 2.46 (s, 4H), 2.32 (s, 3H), 2.21 (s, 3H). HRMS (ESI): calcd. for *m/z* C<sub>16</sub>H<sub>20</sub>ClN<sub>7</sub>O<sub>2</sub>, [M + H]<sup>+</sup> 378.1440, found 378.1440. HPLC (100% MeOH): *t*<sub>R</sub> = 6.251 min, 97.99%.

*N*-(2-(4-Methylpiperazin-1-yl)-5-nitrophenyl)pyrimidin-2-amine (**20**). Yield: 57%. mp 195–197 °C. <sup>1</sup>H NMR (300 MHz, CDCl<sub>3</sub>): δ 9.47 (s, 1H), 8.54 (d, *J* = 3.0 Hz, 2H), 8.03 (s, 1H), 7.88 (d, *J* = 3.0 Hz, 1H), 7.22 (d, *J* = 9.0 Hz, 1H), 6.85 (t, *J* = 9.0 Hz, 1H), 3.04 (t, *J* = 5.6 Hz, 4H), 2.70 (br s, 4H), 2.42 (s, 3H). HRMS (ESI): calcd. for *m/z* C<sub>15</sub>H<sub>18</sub>ClN<sub>7</sub>O<sub>2</sub>, [M + H]<sup>+</sup> 315.1564, found 315.1566. HPLC (100% MeOH): *t*<sub>R</sub> = 16.340 min, 96.09%.

*N*<sup>2</sup>-(2-(4-methylpiperazin-1-yl)-5-nitrophenyl)pyrimidine-2,4-diamine (**21**). Yield: 46%. mp 210–212 °C. <sup>1</sup>H NMR (300 MHz, DMSO-*d*<sub>6</sub>): δ 9.30 (s, 1H), 7.94 (d, *J* = 6.0 Hz, 1H), 7.80 (dd, *J* = 8.7 Hz, 1H), 7.63 (s, 1H), 7.32 (d, *J* = 8.8 Hz, 1H), 6.81 (br s, 2H), 6.03 (d, *J* = 5.8 Hz, 1H), 2.93 (t, *J* = 4.7 Hz, 4H), 2.54 (br s, 4H), 2.26 (s, 3H). HRMS (ESI): calcd. for *m/z* C<sub>15</sub>H<sub>19</sub>N<sub>7</sub>O<sub>2</sub>, [M + H]<sup>+</sup> 330.1673, found 330.1679. HPLC (100% MeOH): *t*<sub>R</sub> = 6.354 min, 96.85%.

#### General Procedure for the Synthesis of 10–12.

Compound **9** (0.35 mmol) was dissolved in the solution of DMF (5 mL) and DIPEA (3 mmol) before the addition of different amines (1 mmol). The reaction was carried out at 120 °C for 4 h. The reaction mixture was subsequently diluted with EA (20 mL) and washed with water (10 mL × 3) and a saturated sodium chloride solution (10 mL). The organic layer was then separated, dried with sodium sulfate (Na<sub>2</sub>SO<sub>4</sub>), filtered, and concentrated to provide crude products. The purified products **10–12** were obtained by column chromatography (DCM/MeOH = 50:1) to afford yellow solids.

*N*<sup>4</sup>,*N*<sup>4</sup>-Dimethyl-*N*<sup>6</sup>-(2-(4-methylpiperazin-1-yl)-5-nitrophenyl)pyrimidine-4,6-diamine (**10**). Yield: 49%. mp 152–154 °C. <sup>1</sup>H NMR (300 MHz, CDCl<sub>3</sub>): δ 8.69 (d, *J* = 2.7 Hz, 1H), 8.28 (s, 1H), 7.80 (dd, *J* = 8.7, 2.7 Hz, 1H), 7.06 (d, *J* = 8.8 Hz, 1H), 6.94 (s, 1H), 5.82 (s, 1H), 3.03 (s, 6H), 2.94 (t, *J* = 4.8 Hz, 4H), 2.65–2.48 (m, 4H), 2.30 (s, 3H). HRMS (ESI): calcd. for *m/z* C<sub>17</sub>H<sub>23</sub>N<sub>7</sub>O<sub>2</sub>, [M + H]<sup>+</sup> 358.1986, found 358.1992. HPLC (100% MeOH): *t*<sub>R</sub> = 4.759 min, 99.20%.

6-(Azetidin-1-yl)-*N*-(2-(4-methylpiperazin-1-yl)-5-nitrophenyl)pyrimidin-4-amine (**11**). Yield: 51%. mp 209–211 °C. <sup>1</sup>H NMR (300 MHz, CDCl<sub>3</sub>): δ 8.64 (d, *J* = 2.7 Hz,



1H), 8.26 (s, 1H), 7.81 (dd,  $J = 8.8, 2.6$  Hz, 1H), 7.06 (d,  $J = 8.8$  Hz, 1H), 6.95 (s, 1H), 5.54 (s, 1H), 4.03 (t,  $J = 7.5$  Hz, 4H), 2.93 (t,  $J = 4.9$  Hz, 4H), 2.55 (d,  $J = 5.2$  Hz, 4H), 2.43 (q,  $J = 7.5$  Hz, 2H), 2.30 (s, 3H). HRMS (ESI): calcd. for  $m/z$   $C_{18}H_{23}N_7O_2$ ,  $[M + H]^+$  370.1986, found 370.1993. HPLC (100% MeOH):  $t_R = 5.293$  min, 96.43%.

**6-Cyclopentyl-N-(2-(4-methylpiperazin-1-yl)-5-nitrophenyl)pyrimidin-4-amine (12).** Yield: 47%. mp 223–225 °C.  $^1H$  NMR (300 MHz,  $CDCl_3$ ):  $\delta$  8.74 (d,  $J = 2.6$  Hz, 1H), 8.36 (s, 1H), 7.89 (dd,  $J = 8.8, 2.7$  Hz, 1H), 7.14 (d,  $J = 8.8$  Hz, 1H), 7.00 (s, 1H), 5.80 (s, 1H), 3.49 (s, 4H), 3.03 (t,  $J = 4.8$  Hz, 4H), 2.64 (s, 4H), 2.39 (s, 3H), 2.03 (s, 4H). HRMS (ESI): calcd. for  $m/z$   $C_{19}H_{26}N_7O_2$ ,  $[M + H]^+$  384.2142, found 384.2154. HPLC (100% MeOH):  $t_R = 9.383$  min, 99.41%.

**6-Chloro- $N^4$ -(5-nitro-2-(piperazin-1-yl)phenyl)pyrimidine-4,5-diamine (23).** 67f (0.35 mmol) was dissolved in the solution of DMF (5 mL) and DIPEA (3 mmol). Then, *tert*-butyl-piperazine-1-carboxylate (1 mmol) was added. The reaction was carried out at 50 °C for 5 h. The reaction mixture was subsequently diluted with EA (20 mL), then washed with water (10 mL  $\times$  3) and a saturated sodium chloride solution (10 mL). The organic layer was then separated, dried by sodium sulfate ( $Na_2SO_4$ ), filtered, and concentrated to provide the crude product. The obtained intermediate was dissolved in the solution of DCM/MeOH (20 mL, 2:1). Then, TFA (2 mL) was dropped. The mixture was stirred at room temperature for 2 h. The mixture was neutralized with a saturated sodium bicarbonate solution and extracted with EA (10 mL  $\times$  3). The organic layer was collected to be concentrated by a rotary evaporator and then washed with  $CH_3CN$  to afford the crude product as a yellow solid, yield: 66%. mp >250 °C.  $^1H$  NMR (300 MHz,  $DMSO-d_6$ ):  $\delta$  9.09 (br s, 1H), 8.60 (d,  $J = 2.7$  Hz, 1H), 8.33 (s, 1H), 7.89 (dd,  $J = 8.9, 2.7$  Hz, 1H), 7.83 (s, 1H), 7.23 (d,  $J = 8.9$  Hz, 1H), 5.55 (s, 2H), 3.21 (s, 4H), 3.42 (t,  $J = 6.0$  Hz, 4H). HRMS (ESI): calcd. for  $m/z$   $C_{14}H_{17}ClN_7O_2$ ,  $[M + H]^+$  350.1127, found 350.1131. HPLC (100% MeOH):  $t_R = 4.069$  min, 96.17%.

**6-Chloro- $N^4$ -(2-morpholino-5-nitrophenyl)pyrimidine-4,5-diamine (24).** The same procedure as 23. Yellow solid, yield: 71%. mp >250 °C.  $^1H$  NMR (300 MHz,  $DMSO-d_6$ ):  $\delta$  8.70 (s, 1H), 8.32 (s, 1H), 8.08–7.86 (m, 2H), 7.29 (d,  $J = 9.0$  Hz, 1H), 5.46 (s, 2H), 3.73 (s, 4H), 2.99 (s, 4H). HRMS (ESI): calcd. for  $m/z$   $C_{14}H_{16}ClN_6O_3$ ,  $[M + H]^+$  351.0967, found 351.0967. HPLC (100% MeOH):  $t_R = 7.041$  min, 98.84%.

**6-Chloro- $N^4$ -(2-(4-ethylpiperazin-1-yl)-5-nitrophenyl)pyrimidine-4,5-diamine (25).** The same procedure as 23. Yellow solid, yield: 47%. mp 185–187 °C.  $^1H$  NMR (300 MHz,  $CDCl_3$ ):  $\delta$  9.34 (s, 1H), 8.32 (s, 1H), 8.18 (s, 1H), 7.93 (dt,  $J = 8.8, 2.7$  Hz, 1H), 7.27–7.20 (m, 1H), 3.60 (s, 2H), 3.08–2.93 (m, 4H), 2.70 (s, 4H), 2.53 (qd,  $J = 7.2, 2.7$  Hz, 2H), 1.16 (td,  $J = 7.3, 2.7$  Hz, 3H). HRMS (ESI): calcd. for  $m/z$   $C_{16}H_{21}ClN_7O_2$ ,  $[M + H]^+$  378.1440, found 378.1449. HPLC (100% MeOH):  $t_R = 4.542$  min, 97.65%.

**6-Chloro- $N^4$ -(2-(4-cyclopropylpiperazin-1-yl)-5-nitrophenyl)pyrimidine-4,5-diamine (26).** The same procedure as 23. Yellow solid, yield: 59%. mp 223–225 °C.  $^1H$  NMR (300 MHz,  $CDCl_3$ ):  $\delta$  9.35 (d,  $J = 2.7$  Hz, 1H), 8.32 (s, 1H), 8.21 (s, 1H), 7.92 (dd,  $J = 8.7, 2.7$  Hz, 1H), 7.22 (d,  $J = 8.8$  Hz, 1H), 3.62 (s, 2H), 2.96 (t,  $J = 4.7$  Hz, 4H), 2.87 (s, 4H), 1.78–1.71 (m, 1H), 0.56–0.51 (m, 2H), 0.49–0.44 (m, 2H). HRMS (ESI): calcd. for  $m/z$   $C_{17}H_{21}ClN_7O_2$ ,  $[M + H]^+$

390.1440, found 390.1446. HPLC (100% MeOH):  $t_R = 4.811$  min, 99.31%.

**2-(4-(2-((5-Amino-6-chloropyrimidin-4-yl)amino)-4-nitrophenyl)piperazin-1-yl)ethan-1-ol (27).** The same procedure as 23. Yellow solid, yield: 76%. mp 202–204 °C.  $^1H$  NMR (300 MHz,  $CDCl_3$ ):  $\delta$  9.33 (s, 1H), 8.32 (s, 1H), 8.15 (s, 1H), 7.94 (d,  $J = 8.7$  Hz, 1H), 7.27 (s, 1H), 3.70 (s, 2H), 3.64–2.46 (m, 2H), 3.02 (s, 4H), 2.78 (s, 4H), 2.68 (s, 2H), 2.57 (s, 1H). HRMS (ESI): calcd. for  $m/z$   $C_{16}H_{20}ClN_7O_3$ ,  $[M + H]^+$  394.1389, found 394.1387. HPLC (100% MeOH):  $t_R = 7.347$  min, 96.12%.

**6-Chloro- $N^4$ -(5-nitro-2-(4-phenylpiperazin-1-yl)phenyl)pyrimidine-4,5-diamine (28).** The same procedure as 23. Yellow solid: yield 76%. mp >250 °C.  $^1H$  NMR (300 MHz,  $CDCl_3$ ):  $\delta$  9.39 (d,  $J = 2.7$  Hz, 1H), 8.35 (s, 1H), 8.25 (s, 1H), 7.97 (dd,  $J = 8.9, 2.6$  Hz, 1H), 7.39–7.28 (m, 3H), 7.06–6.90 (m, 3H), 3.54 (s, 2H), 3.44 (t,  $J = 4.9$  Hz, 4H), 3.16 (t,  $J = 4.9$  Hz, 4H). HRMS (ESI): calcd. for  $m/z$   $C_{20}H_{20}ClN_7O_2$ ,  $[M + H]^+$  426.1440, found 426.1449. HPLC (100% MeOH):  $t_R = 4.905$  min, 95.52%.

#### General Procedure for the Synthesis of Compounds

**29–32.** 70 (1.0 g, 2.5 mmol) was dissolved in the solution of dioxane (30 mL), and different boronic acids (1.2 equiv) were added to the solution. Then,  $Cs_2CO_3$  (1.6 g, 5 mmol) and a catalytic amount of  $Pd(PPh_3)_2Cl_2$  were added to the mixture. The reaction bottle was protected with  $N_2$ , and the mixture was refluxed for 20 h. The solution was filtered to remove the catalytic agent and  $Cs_2CO_3$ , then purified by column chromatography on silica gel using a common 1–5% MeOH/DCM gradient to afford compounds 29–32 as light yellow solids.

**$N^4$ -(4'-Amino-4-(4-methylpiperazin-1-yl)-[1,1'-biphenyl]-3-yl)-6-chloropyrimidine-4,5-diamine (29).** Yield: 67%. mp 212–214 °C.  $^1H$  NMR (300 MHz,  $DMSO-d_6$ ):  $\delta$  8.16 (d,  $J = 8.1$  Hz, 2H), 7.90 (s, 1H), 7.65 (d,  $J = 8.2$  Hz, 2H), 7.55 (d,  $J = 8.4$  Hz, 2H), 7.37 (d,  $J = 8.4$  Hz, 1H), 7.26 (d,  $J = 8.2$  Hz, 1H), 5.43 (s, 2H), 5.15 (s, 2H), 3.17 (s, 4H), 3.06 (s, 4H), 2.75 (s, 3H).  $m/z$  (EI-MS): 410.2  $[M]^+$ . HPLC (100% methanol):  $t_R = 7.489$  min, 95.67%.

**6-Chloro- $N^4$ -(4'-methoxy-4-(4-methylpiperazin-1-yl)-[1,1'-biphenyl]-3-yl)pyrimidine-4,5-diamine (30).** Yield: 60%. mp 211–213 °C.  $^1H$  NMR (300 MHz,  $DMSO-d_6$ ):  $\delta$  8.24 (s, 2H), 7.90 (s, 1H), 7.57 (d,  $J = 7.9$  Hz, 2H), 7.40–7.35 (m, 3H), 7.24 (d,  $J = 8.3$  Hz, 1H), 5.37 (s, 2H), 5.22 (s, 1H), 4.52 (s, 2H), 2.85 (t,  $J = 4.5$  Hz, 4H), 2.53 (s, 4H), 2.24 (s, 3H). (EI-MS):  $m/z$  425.2  $[M]^+$ . HPLC (80% methanol in water):  $t_R = 4.590$  min, 99.44%.

**6-Chloro- $N^4$ -(2-(4-methylpiperazin-1-yl)-5-(pyrimidin-5-yl)phenyl)pyrimidine-4,5-diamine (31).** Yield: 46%. mp 189–191 °C.  $^1H$  NMR (300 MHz,  $DMSO-d_6$ ):  $\delta$  9.17 (s, 1H), 9.10 (s, 2H), 8.57 (s, 1H), 7.80 (s, 1H), 7.10 (dd,  $J = 7.5, 2.0$  Hz, 1H), 6.99 (d,  $J = 7.4$  Hz, 1H), 6.82 (d,  $J = 2.0$  Hz, 1H), 5.32 (s, 2H), 2.85 (s, 4H), 2.54 (s, 4H), 2.34 (s, 3H). HRMS (ESI): calcd. for  $m/z$   $C_{19}H_{22}ClN_8$ ,  $[M + H]^+$  397.1651, found 397.1653. HPLC (80% methanol in water):  $t_R = 3.973$  min, 97.50%.

**6-Chloro- $N^4$ -(5-(furan-3-yl)-2-(4-methylpiperazin-1-yl)-phenyl)pyrimidine-4,5-diamine (32).** Yield: 70%. mp 164–166 °C.  $^1H$  NMR (300 MHz,  $DMSO-d_6$ ):  $\delta$  8.23 (s, 1H), 7.90 (s, 1H), 7.54 (d,  $J = 7.5$  Hz, 1H), 7.43 (s, 1H), 7.07 (d,  $J = 7.7$  Hz, 1H), 6.91 (d,  $J = 7.4$  Hz, 1H), 6.82 (s, 1H), 6.53 (d,  $J = 8.0$  Hz, 1H), 5.36 (s, 2H), 2.85 (s, 4H), 2.61 (s, 4H), 2.25 (s, 3H). HRMS (ESI): calcd. for  $m/z$   $C_{19}H_{22}ClN_6O$ ,  $[M + H]^+$

385.1538, found 385.1538. HPLC (90% methanol in water):  $t_R$  = 6.859 min, 96.26%.

**General Procedure for the Synthesis of Compounds 34–38.** To a solution of different acids (0.35 mmol) in DMF (8 mL) at room temperature was added the BOP reagent (0.26 g, 0.59 mmol), followed by  $\text{Et}_3\text{N}$  (0.1 mL, 0.88 mmol). The mixture was stirred for 0.5 h before compound **29** (0.12 g, 0.29 mmol) was added. Then, the mixture was stirred at room temperature for 12 h. The aqueous solution was poured into 50 mL of water and extracted with EA ( $3 \times 50$  mL), and the organic phase was dried over  $\text{Na}_2\text{SO}_4$ , filtered, and concentrated to obtain the crude product, which was then purified by column chromatography on silica gel using a common 1–5% MeOH/DCM gradient to afford compounds **34–38** as light yellow solids.

**N-(3'-((5-Amino-6-chloropyrimidin-4-yl)amino)-4'-(4-methylpiperazin-1-yl)-[1,1'-biphenyl]-4-yl)tetrahydro-2H-pyran-4-carboxamide (34).** Yield: 78%. mp 207–209 °C.  $^1\text{H}$  NMR (300 MHz,  $\text{DMSO}-d_6$ ):  $\delta$  9.99 (s, 1H), 8.21 (s, 1H), 7.90 (s, 1H), 7.68 (dd,  $J$  = 8.4, 5.9 Hz, 3H), 7.57–7.54 (m, 2H), 7.38–7.35 (m, 1H), 7.24–7.22 (m, 1H), 5.38 (s, 2H), 3.94–3.90 (m, 3H), 3.37–3.35 (m, 2H), 2.92 (s, 4H), 2.76 (s, 4H), 2.43 (s, 3H), 1.72–1.69 (m, 4H).  $^{13}\text{C}$  NMR (75 MHz,  $\text{DMSO}-d_6$ ):  $\delta$  173.52, 150.72, 146.29, 142.40, 140.15, 139.15, 136.23, 134.86, 134.03, 127.06, 125.57, 122.34, 121.86, 121.07, 120.00, 66.88, 53.87, 48.83, 42.21, 29.36. HRMS (ESI): calcd. for  $m/z$   $\text{C}_{27}\text{H}_{32}\text{ClN}_7\text{O}_2$ ,  $[\text{M} + \text{H}]^+$  522.2379, found 522.2377. HPLC (80% methanol in water):  $t_R$  = 4.280 min, 95.50%.

**N-(3'-((5-Amino-6-chloropyrimidin-4-yl)amino)-4'-(4-methylpiperazin-1-yl)-[1,1'-biphenyl]-4-yl)-1-methylpiperidine-4-carboxamide (35).** Yield: 64%. mp 157–160 °C.  $^1\text{H}$  NMR (300 MHz,  $\text{DMSO}-d_6$ ):  $\delta$  10.19 (s, 1H), 8.22–8.19 (m, 2H), 7.95 (s, 1H), 7.69 (d,  $J$  = 8.4 Hz, 2H), 7.57 (d,  $J$  = 8.7 Hz, 2H), 7.36 (d,  $J$  = 8.4 Hz, 1H), 7.24 (d,  $J$  = 8.1 Hz, 1H), 5.42 (s, 2H), 2.99–2.90 (m, 5H), 2.85 (s, 4H), 2.73 (s, 3H), 2.53 (s, 4H), 2.49 (s, 3H), 2.03–1.99 (m, 4H). HRMS (ESI): calcd. for  $m/z$   $\text{C}_{28}\text{H}_{36}\text{ClN}_8\text{O}$ ,  $[\text{M} + \text{H}]^+$  535.2695, found 535.2710. HPLC (80% methanol in water):  $t_R$  = 4.518 min, 98.25%.

**N-(3'-((5-Amino-6-chloropyrimidin-4-yl)amino)-4'-(4-methylpiperazin-1-yl)-[1,1'-biphenyl]-4-yl)-cyclohexanecarboxamide (36).** Yield: 80%. mp 256–258 °C.  $^1\text{H}$  NMR (300 MHz,  $\text{DMSO}-d_6$ ):  $\delta$  9.91 (s, 1H), 8.18 (d,  $J$  = 8.2 Hz, 2H), 7.90 (s, 1H), 7.69 (d,  $J$  = 8.3 Hz, 2H), 7.55 (d,  $J$  = 8.4 Hz, 2H), 7.37 (d,  $J$  = 8.4 Hz, 1H), 7.26 (d,  $J$  = 8.2 Hz, 1H), 5.43 (s, 2H), 3.17 (s, 4H), 3.06 (s, 4H), 2.75 (s, 3H), 2.34–2.30 (m, 1H), 1.76 (t,  $J$  = 12.5 Hz, 4H), 1.42 (t,  $J$  = 11.6 Hz, 2H), 1.33–1.09 (m, 4H). HRMS (ESI): calcd. for  $m/z$   $\text{C}_{28}\text{H}_{34}\text{ClN}_7\text{O}$ ,  $[\text{M} + \text{H}]^+$  520.2586, found 520.2584. HPLC (90% methanol in water):  $t_R$  = 4.003 min, 97.87%.

**N-(3'-((5-Amino-6-chloropyrimidin-4-yl)amino)-4'-(4-methylpiperazin-1-yl)-[1,1'-biphenyl]-4-yl)butyramide (37).** Yield: 80%. mp 196–198 °C.  $^1\text{H}$  NMR (300 MHz,  $\text{DMSO}-d_6$ ):  $\delta$  10.00 (s, 1H), 8.21–8.16 (m, 2H), 7.90 (d,  $J$  = 6.0 Hz, 1H), 7.71–7.69 (m, 2H), 7.59–7.54 (m, 2H), 7.38 (d,  $J$  = 7.8 Hz, 1H), 7.27 (d,  $J$  = 8.2 Hz, 1H), 5.44 (s, 2H), 3.51–3.46 (m, 4H), 3.27–3.16 (m, 4H), 2.88 (s, 3H), 2.32–2.27 (m, 2H), 1.68–1.58 (m, 2H), 0.96–0.89 (m, 3H). HRMS (ESI): calcd. for  $m/z$   $\text{C}_{25}\text{H}_{31}\text{ClN}_7\text{O}$ ,  $[\text{M} + \text{H}]^+$  480.2273, found 480.2274. HPLC (80% methanol in water):  $t_R$  = 4.696 min, 96.97%.

**N-(3'-((5-Amino-6-chloropyrimidin-4-yl)amino)-4'-(4-methylpiperazin-1-yl)-[1,1'-biphenyl]-4-yl)benzamide (38).** Yield: 78%. mp >250 °C.  $^1\text{H}$  NMR (300 MHz,  $\text{DMSO}-d_6$ ):

$\delta$  10.00 (s, 1H), 8.21–8.16 (m, 2H), 7.90 (d,  $J$  = 6.0 Hz, 1H), 7.71–7.69 (m, 2H), 7.59–7.54 (m, 2H), 7.38 (d,  $J$  = 7.8 Hz, 1H), 7.27 (d,  $J$  = 8.2 Hz, 1H), 5.44 (s, 2H), 3.51–3.46 (m, 4H), 3.27–3.16 (m, 4H), 2.88 (s, 3H), 2.32–2.27 (m, 2H), 1.68–1.58 (m, 2H), 0.96–0.89 (m, 3H).  $^{13}\text{C}$  NMR (75 MHz,  $\text{DMSO}-d_6$ ):  $\delta$  166.01, 151.06, 146.61, 143.61, 140.32, 138.84, 135.73, 135.52, 135.42, 133.91, 132.05, 128.87, 128.15, 126.97, 125.53, 122.22, 121.30, 121.19, 120.73, 55.53, 51.51, 46.32. HRMS (ESI): calcd. for  $m/z$   $\text{C}_{28}\text{H}_{28}\text{ClN}_7\text{O}$ ,  $[\text{M} + \text{H}]^+$  514.2117, found 514.2115. HPLC (90% methanol in water):  $t_R$  = 3.889 min, 95.09%.

**Methyl 1-(3-((5-Amino-6-chloropyrimidin-4-yl)amino)-4-(4-methylpiperazin-1-yl) phenyl)-1H-1,2,3-triazole-4-carboxylate (33).** **33** was prepared from **74** and 4,6-dichloro-5-nitropyrimidine according to the procedure of **70**. Yield: 66%. mp 231–233 °C.  $^1\text{H}$  NMR (300 MHz,  $\text{DMSO}-d_6$ ):  $\delta$  9.46 (s, 1H), 8.62 (s, 1H), 8.34 (s, 1H), 7.95 (s, 1H), 7.64 (d,  $J$  = 8.6 Hz, 1H), 7.37 (d,  $J$  = 8.7 Hz, 1H), 5.44 (s, 2H), 3.89 (s, 3H), 2.88 (s, 4H), 2.51 (s, 4H), 2.23 (s, 3H). HRMS (ESI): calcd. for  $m/z$   $\text{C}_{19}\text{H}_{22}\text{ClFN}_9\text{O}_2$ ,  $[\text{M} + \text{H}]^+$  444.1657, found 444.1660. HPLC (90% methanol in water):  $t_R$  = 3.775 min, 97.63%.

**Methyl 4'-Fluoro-3'-nitro-[1,1'-biphenyl]-4-carboxylate (75).** 4-Bromo-1-fluoro-2-nitrobenzene (5.0 g, 22.8 mmol) was dissolved in the solution of dioxane (150 mL) before the addition of boronic acid (27.3 mmol). Then,  $\text{Cs}_2\text{CO}_3$  (14.8 g, 45.6 mmol) and a catalytic amount of  $\text{Pd}(\text{PPh}_3)_2\text{Cl}_2$  were added. The mixture was protected with  $\text{N}_2$  and then refluxed for 20 h. The solution was filtered to remove the catalytic agent and  $\text{Cs}_2\text{CO}_3$ , then purified by column chromatography on silica gel using a common 1–5% MeOH/DCM gradient to afford intermediate **75**. Yield: 70%. mp 145–147 °C.  $^1\text{H}$  NMR (300 MHz,  $\text{CDCl}_3$ ):  $\delta$  8.31–8.13 (m, 3H), 7.88–7.59 (m, 1H), 8.28 (m, 3H), 7.42–7.36 (m, 1H), 3.94 (s, 3H). (EI-MS):  $m/z$  276.2  $[\text{M}]^+$ .

**Methyl 3'-Amino-4'-(4-methylpiperazin-1-yl)-[1,1'-biphenyl]-4-carboxylate (76).** **76** was prepared from **75** similar to intermediate **69**. Yield: 90%. mp 229–231 °C.  $^1\text{H}$  NMR (300 MHz,  $\text{CDCl}_3$ ):  $\delta$  8.07 (d,  $J$  = 8.5 Hz, 2H), 7.61 (dd,  $J$  = 6.7, 1.8 Hz, 2H), 7.09 (d,  $J$  = 8.5 Hz, 1H), 7.03 (m, 2H), 4.06 (s, 2H), 3.93 (s, 3H), 3.01 (t,  $J$  = 4.4 Hz, 4H), 2.61 (s, 4H), 2.38 (s, 3H). (EI-MS):  $m/z$  326.2  $[\text{M}]^+$ .

**Methyl 3'-((5-Amino-6-chloropyrimidin-4-yl)amino)-4'-(4-methylpiperazin-1-yl)-[1,1'-biphenyl]-4-carboxylate (77).** The same procedure as that for **33** was used. Yield: 46%. mp 209–210 °C.  $^1\text{H}$  NMR (300 MHz,  $\text{DMSO}-d_6$ ):  $\delta$  8.53–8.42 (m, 1H), 8.23 (s, 1H), 7.96–7.90 (m, 3H), 7.70 (d,  $J$  = 8.4 Hz, 2H), 7.46–7.42 (m, 1H), 7.26 (d,  $J$  = 8.3 Hz, 1H), 5.36 (s, 2H), 3.93 (s, 3H), 3.57 (t,  $J$  = 4.6 Hz, 4H), 2.87 (t,  $J$  = 4.7 Hz, 4H), 2.24 (s, 3H). (EI-MS):  $m/z$  453.2  $[\text{M}]^+$ .

**General Procedure for Preparation of Compounds 39–48.** The ester group was hydrolyzed by LiOH in MeOH/ $\text{H}_2\text{O}$  to give the acid intermediate. Then, the BOP reagent (0.22 g, 0.49 mmol) was added to a solution of acid (0.1 g, 0.26 mmol) in DMF (10 mL) at room temperature, followed by TEA (0.12 mL, 0.88 mmol). Then, different amines (0.39 mmol) were added to reaction mixture, and the mixture was stirred for 30 min. Then, the resultant solution was stirred at room temperature for 12 h. The mixture was poured into 50 mL of water and extracted with EA ( $3 \times 50$  mL). The organic layer was dried by  $\text{Na}_2\text{SO}_4$ , filtered, and concentrated by a rotary evaporator below 50 °C under reduced pressure to obtain the crude products. The final products were purified by column chromatography on silica gel using a common 1–10%



MeOH/DCM gradient to afford compounds **39–48** as white solids.

**3'-((5-Amino-6-chloropyrimidin-4-yl)amino)-4'-(4-methylpiperazin-1-yl)-[1,1'-biphenyl]-4-yl(morpholino)methanone (39).** Yield: 68%. mp 225–227 °C. <sup>1</sup>H NMR (300 MHz, DMSO-*d*<sub>6</sub>): δ 8.45 (d, *J* = 13.6 Hz, 2H), 7.90 (s, 1H), 7.69 (d, *J* = 7.9 Hz, 2H), 7.49 (d, *J* = 7.7 Hz, 2H), 7.42 (d, *J* = 8.4 Hz, 1H), 7.27 (d, *J* = 8.2 Hz, 1H), 5.39 (s, 2H), 3.61 (s, 4H), 3.35 (s, 4H), 2.98–2.90 (s, 4H), 2.64 (s, 4H), 2.34 (s, 3H). HRMS (ESI): calcd. for *m/z* C<sub>26</sub>H<sub>30</sub>ClN<sub>7</sub>O<sub>2</sub>, [M + H]<sup>+</sup> 508.2222, found 508.2223. HPLC (80% methanol in water): *t*<sub>R</sub> = 3.507 min, 98.81%.

**3'-((5-Amino-6-chloropyrimidin-4-yl)amino)-4'-(4-methylpiperazin-1-yl)-N-(2-morpholinoethyl)-[1,1'-biphenyl]-4-carboxamide (40).** Yield: 56%. mp 230–232 °C. <sup>1</sup>H NMR (300 MHz, DMSO-*d*<sub>6</sub>): δ 8.45 (s, 1H), 8.27–8.22 (m, 2H), 7.92–7.90 (m, 3H), 7.71 (d, *J* = 8.0 Hz, 2H), 7.45 (d, *J* = 8.2 Hz, 1H), 7.26 (d, *J* = 8.4 Hz, 1H), 5.39 (s, 2H), 3.58 (s, 4H), 3.40–3.34 (m, 4H), 2.90 (s, 4H), 2.61 (s, 4H), 2.44 (s, 4H), 2.31 (s, 3H). HRMS (ESI): calcd. for *m/z* C<sub>28</sub>H<sub>35</sub>ClN<sub>8</sub>O<sub>2</sub>, [M + H]<sup>+</sup> 551.2644, found 551.2639. HPLC (80% methanol in water): *t*<sub>R</sub> = 3.196 min, 98.91%.

**3'-((5-Amino-6-chloropyrimidin-4-yl)amino)-4'-(4-methylpiperazin-1-yl)-N-(3-morpholinopropyl)-[1,1'-biphenyl]-4-carboxamide (41).** Yield: 49%. mp 210–212 °C. <sup>1</sup>H NMR (300 MHz, DMSO-*d*<sub>6</sub>): δ 8.53–8.42 (m, 1H), 8.28 (d, *J* = 2.8 Hz, 1H), 8.23 (s, 1H), 7.96–7.90 (m, 3H), 7.70 (d, *J* = 8.4 Hz, 2H), 7.46–7.42 (m, 1H), 7.26 (d, *J* = 8.3 Hz, 1H), 5.36 (s, 2H), 3.57 (t, *J* = 4.6 Hz, 4H), 3.32–3.30 (m, 2H), 2.87 (t, *J* = 4.7 Hz, 4H), 2.51–2.49 (m, 4H), 2.37–2.32 (m, 6H), 2.24 (s, 3H), 1.74–1.70 (m, 2H). HRMS (ESI): calcd. for *m/z* C<sub>29</sub>H<sub>37</sub>ClN<sub>8</sub>O<sub>2</sub>, [M + H]<sup>+</sup> 565.2801, found 565.2801. HPLC (80% methanol in water): *t*<sub>R</sub> = 3.947 min, 96.00%.

**3'-((5-Amino-6-chloropyrimidin-4-yl)amino)-4'-(4-methylpiperazin-1-yl)-N-(tetrahydro-2H-pyran-4-yl)-[1,1'-biphenyl]-4-carboxamide (42).** Yield: 76%. mp 218–220 °C. <sup>1</sup>H NMR (300 MHz, DMSO-*d*<sub>6</sub>): δ 8.35 (d, *J* = 7.7 Hz, 1H), 8.26 (s, 1H), 8.20 (s, 1H), 8.01–7.82 (m, 3H), 7.71 (d, *J* = 8.2 Hz, 2H), 7.46 (d, *J* = 8.1 Hz, 1H), 7.28 (d, *J* = 8.4 Hz, 1H), 5.44 (s, 2H), 4.01 (s, 1H), 3.88 (d, *J* = 10.5 Hz, 2H), 3.42–3.34 (m, 4H), 3.00 (s, 6H), 2.51 (s, 3H), 1.90–1.78 (m, 2H), 1.60–1.56 (m, 2H). <sup>13</sup>C NMR (75 MHz, DMSO-*d*<sub>6</sub>): δ 165.68, 158.03, 150.68, 146.29, 142.80, 140.19, 133.91, 133.69, 128.48, 126.54, 125.59, 122.98, 122.34, 121.04, 66.66, 54.46, 46.22, 32.92. HRMS (ESI): calcd. for *m/z* C<sub>27</sub>H<sub>32</sub>ClN<sub>7</sub>O<sub>2</sub>, [M + H]<sup>+</sup> 522.2379, found 522.2379. HPLC (80% methanol in water): *t*<sub>R</sub> = 4.383 min, 95.49%.

**3'-((5-Amino-6-chloropyrimidin-4-yl)amino)-N,N-dimethyl-4'-(4-methylpiperazin-1-yl)-[1,1'-biphenyl]-4-carboxamide (43).** Yield: 79%. mp 142–145 °C. <sup>1</sup>H NMR (300 MHz, DMSO-*d*<sub>6</sub>): δ 8.24 (s, 1H), 7.70 (s, 2H), 7.56–7.41 (m, 5H), 7.02 (s, 1H), 5.57 (s, 2H), 3.19–2.97 (m, 10H), 2.75 (s, 4H), 2.43 (s, 3H). HRMS (ESI): calcd. for *m/z* C<sub>24</sub>H<sub>28</sub>ClN<sub>7</sub>O, [M + H]<sup>+</sup> 466.2117, found 466.2121. HPLC (80% methanol in water): *t*<sub>R</sub> = 2.489 min, 95.56%.

**3'-((5-Amino-6-chloropyrimidin-4-yl)amino)-4'-(4-methylpiperazin-1-yl)-[1,1'-biphenyl]-4-yl(4-methylpiperazin-1-yl)methanone (44).** Yield: 57%. mp >250 °C. <sup>1</sup>H NMR (300 MHz, DMSO-*d*<sub>6</sub>): δ 8.54 (d, *J* = 13.6 Hz, 2H), 7.90 (s, 1H), 7.68 (d, *J* = 7.9 Hz, 2H), 7.45 (d, *J* = 7.7 Hz, 2H), 7.39 (d, *J* = 8.4 Hz, 1H), 7.27 (d, *J* = 8.1 Hz, 1H), 5.35 (s, 2H), 3.61 (s, 4H), 3.35 (s, 4H), 2.98–2.90 (s, 4H), 2.64 (s, 4H), 2.34 (s, 3H), 2.30 (s, 3H). HRMS (ESI): calcd. for *m/z* C<sub>27</sub>H<sub>33</sub>ClN<sub>8</sub>O,

[M + H]<sup>+</sup> 521.2937, found 521.2937. HPLC (80% methanol in water): *t*<sub>R</sub> = 4.094 min, 98.10%.

**3'-((5-Amino-6-chloropyrimidin-4-yl)amino)-4'-(4-methylpiperazin-1-yl)-N-(1-methylpiperidin-4-yl)-[1,1'-biphenyl]-4-carboxamide (45).** Yield: 47%. mp >250 °C. <sup>1</sup>H NMR (300 MHz, DMSO-*d*<sub>6</sub>): δ 8.48 (s, 1H), 8.22 (s, 1H), 8.14 (s, 1H), 7.87 (d, *J* = 7.9 Hz, 2H), 7.77 (s, 1H), 7.61 (d, *J* = 8.0 Hz, 2H), 7.36 (d, *J* = 8.1 Hz, 1H), 7.16 (d, *J* = 7.5 Hz, 1H), 5.40 (s, 2H), 3.92 (s, 1H), 3.22 (s, 4H), 2.87 (s, 4H), 2.64 (s, 2H), 2.41 (s, 6H), 2.30 (s, 2H), 1.86 (s, 4H). HRMS (ESI): calcd. for *m/z* C<sub>28</sub>H<sub>35</sub>ClN<sub>8</sub>O, [M + H]<sup>+</sup> 535.2695, found 535.2700. HPLC (80% methanol in water): *t*<sub>R</sub> = 4.512 min, 97.75%.

**3'-((5-Amino-6-chloropyrimidin-4-yl)amino)-4'-(4-methylpiperazin-1-yl)-[1,1'-biphenyl]-4-yl(4-hydroxycyclohexyl)methanone (46).** Yield: 42%. mp 190–192 °C. <sup>1</sup>H NMR (300 MHz, DMSO-*d*<sub>6</sub>): δ 8.24 (d, *J* = 8.4 Hz, 2H), 7.89 (s, 1H), 7.67 (d, *J* = 7.9 Hz, 2H), 7.50–7.37 (m, 3H), 7.26 (d, *J* = 8.3 Hz, 1H), 5.41 (s, 2H), 4.82 (s, 1H), 3.74 (m, 1H), 3.25–3.16 (m, 4H), 2.92 (m, 4H), 2.68 (s, 4H), 2.36 (s, 3H), 1.75 (s, 2H), 1.35 (s, 2H). <sup>13</sup>C NMR (75 MHz, DMSO-*d*<sub>6</sub>): δ 169.15, 150.72, 146.37, 143.10, 141.25, 140.25, 135.48, 133.96, 127.93, 126.81, 125.58, 122.83, 122.12, 121.07, 65.96, 54.46, 49.62. HRMS (ESI): calcd. for *m/z* C<sub>27</sub>H<sub>32</sub>ClN<sub>7</sub>O<sub>2</sub>, [M + H]<sup>+</sup> 522.2378, found 522.2379. HPLC (90% methanol in water): *t*<sub>R</sub> = 3.965 min, 96.50%.

**3'-((5-Amino-6-chloropyrimidin-4-yl)amino)-4'-(4-methylpiperazin-1-yl)-[1,1'-biphenyl]-4-yl(4-hydroxy-4-methylpiperidin-1-yl)methanone (47).** Yield: 45%. mp 185–187 °C. <sup>1</sup>H NMR (300 MHz, DMSO-*d*<sub>6</sub>): δ 8.16 (s, 2H), 7.80 (s, 1H), 7.57 (d, *J* = 7.9 Hz, 2H), 7.37–7.31 (m, 3H), 7.17 (d, *J* = 8.3 Hz, 1H), 5.34 (s, 2H), 4.37 (s, 1H), 3.23–3.03 (m, 4H), 2.83 (s, 4H), 2.60 (s, 4H), 2.27 (s, 3H), 1.50–1.37 (m, 4H), 1.06 (s, 3H). HRMS (ESI): calcd. for *m/z* C<sub>28</sub>H<sub>34</sub>ClN<sub>7</sub>O<sub>2</sub>, [M + H]<sup>+</sup> 536.2535, found 536.2533. HPLC (80% methanol in water): *t*<sub>R</sub> = 4.567 min, 95.52%.

**3'-((5-Amino-6-chloropyrimidin-4-yl)amino)-N-isopropyl-4'-(4-methylpiperazin-1-yl)-[1,1'-biphenyl]-4-carboxamide (48).** Yield: 64%. mp 184–186 °C. <sup>1</sup>H NMR (300 MHz, DMSO-*d*<sub>6</sub>): δ 8.27–8.22 (m, 2H), 7.91 (d, *J* = 8.1 Hz, 2H), 7.71 (s, 1H), 7.59 (d, *J* = 8.0 Hz, 2H), 7.43–7.30 (m, 2H), 7.04 (d, *J* = 8.2 Hz, 1H), 5.54 (s, 2H), 4.12 (s, 1H), 3.33 (s, 4H), 3.07 (s, 4H), 2.82 (s, 3H), 1.18 (s, 6H). HRMS (ESI): calcd. for *m/z* C<sub>25</sub>H<sub>30</sub>ClN<sub>7</sub>O, [M + H]<sup>+</sup> 480.2279, found 480.2276. HPLC (80% methanol in water): *t*<sub>R</sub> = 3.601 min, 96.77%.

**3'-((5-Amino-6-chloropyrimidin-4-yl)amino)-2'-fluoro-N,N-dimethyl-4'-(4-methylpiperazin-1-yl)-[1,1'-biphenyl]-4-carboxamide (49).** The same procedure as that for **39**. White solid, yield 77%. mp 158–160 °C. <sup>1</sup>H NMR (300 MHz, DMSO-*d*<sub>6</sub>): δ 8.03 (s, 1H), 7.71 (s, 1H), 7.60–7.46 (m, 4H), 7.40 (t, *J* = 8.5 Hz, 1H), 7.00 (d, *J* = 8.6 Hz, 1H), 5.49 (s, 2H), 2.99–2.98 (m, 6H), 2.87 (s, 4H), 2.38 (s, 4H), 2.18 (s, 3H). HRMS (ESI): calcd. for *m/z* C<sub>24</sub>H<sub>27</sub>ClFN<sub>7</sub>O, [M + H]<sup>+</sup> 484.2202, found 484.2203. HPLC (80% methanol in water): *t*<sub>R</sub> = 3.448 min, 95.30%.

**3'-((5-Amino-6-chloropyrimidin-4-yl)amino)-2'-fluoro-4'-(4-methylpiperazin-1-yl)-[1,1'-biphenyl]-4-yl(morpholino)methanone (50).** The same procedure as that for **39**. White solid, yield 85%. mp 145–148 °C. <sup>1</sup>H NMR (300 MHz, DMSO-*d*<sub>6</sub>): δ 8.05 (s, 1H), 7.72 (s, 1H), 7.54 (dd, *J* = 8.5, 5.4 Hz, 4H), 7.41 (t, *J* = 8.5 Hz, 1H), 7.03 (d, *J* = 8.6 Hz, 1H), 5.48 (s, 2H), 3.61 (s, 4H), 3.34 (s, 4H), 2.98 (s, 4H), 2.65 (s, 4H), 2.38 (s, 3H). <sup>13</sup>C NMR (75 MHz, DMSO-*d*<sub>6</sub>): δ

169.20, 156.80, 150.45, 145.58, 138.73, 137.73, 136.78, 134.93, 128.97, 128.95, 127.93, 127.82, 125.43, 121.23, 121.08, 115.70. HRMS (ESI): calcd. for  $m/z$   $C_{26}H_{29}ClFN_7O_2$ ,  $[M + H]^+$  526.2128, found 526.2122. HPLC (80% methanol in water):  $t_R$  = 3.560 min, 98.66%.

**3'-((5-Amino-6-chloropyrimidin-4-yl)amino)-2'-fluoro-4'-(4-methylpiperazin-1-yl)-N-(2-morpholinoethyl)-[1,1'-biphenyl]-4-carboxamide (51).** The same procedure as that for 39. White solid, yield: 75%. mp 199–202 °C.  $^1H$  NMR (300 MHz, DMSO- $d_6$ ):  $\delta$  8.48 (t,  $J$  = 5.5 Hz, 1H), 8.09 (s, 1H), 7.90 (d,  $J$  = 8.1 Hz, 2H), 7.71 (s, 1H), 7.59 (d,  $J$  = 7.9 Hz, 2H), 7.41 (t,  $J$  = 8.5 Hz, 1H), 7.00 (d,  $J$  = 8.5 Hz, 1H), 5.50 (s, 2H), 3.57 (s, 4H), 3.41–3.38 (m, 2H), 2.91 (s, 4H), 2.49 (s, 4H), 2.42 (s, 6H), 2.21 (s, 3H).  $^{13}C$  NMR (75 MHz, DMSO- $d_6$ ):  $\delta$  167.95, 166.21, 150.46, 149.96, 145.53, 138.60, 138.27, 133.78, 128.80, 127.90, 125.45, 116.36, 115.49, 99.99, 66.63, 65.69, 57.81, 54.94, 53.74, 50.43, 37.00. HRMS (ESI): calcd. for  $m/z$   $C_{28}H_{34}ClFN_8O_2$ ,  $[M + H]^+$  569.2550, found 569.2548. HPLC (80% methanol in water):  $t_R$  = 3.634 min, 98.88%.

**3'-((5-Amino-6-chloropyrimidin-4-yl)amino)-2'-fluoro-4'-(4-methylpiperazin-1-yl)-N-(3-morpholinopropyl)-[1,1'-biphenyl]-4-carboxamide (52).** The same procedure as that for 39. White solid, yield: 65%. mp 202–205 °C.  $^1H$  NMR (300 MHz, DMSO- $d_6$ ):  $\delta$  8.46 (t,  $J$  = 5.7 Hz, 1H), 7.96 (s, 1H), 7.81 (d,  $J$  = 8.2 Hz, 2H), 7.31 (t,  $J$  = 8.6 Hz, 2H), 6.90 (d,  $J$  = 8.7 Hz, 1H), 5.40 (s, 2H), 3.47 (t,  $J$  = 5.4 Hz, 4H), 3.21–3.19 (m, 2H), 2.80 (s, 4H), 2.28–2.22 (m, 10H), 2.09 (s, 3H), 1.60 (t,  $J$  = 7.1 Hz, 2H).  $^{13}C$  NMR (75 MHz, DMSO- $d_6$ ):  $\delta$  166.21, 154.80, 150.45, 149.97, 145.55, 138.63, 138.21, 133.89, 128.77, 127.88, 125.44, 124.46, 124.21, 122.23, 122.13, 121.16, 121.05, 115.46, 66.59, 56.48, 54.99, 53.76, 50.51, 46.02, 38.19, 26.38. HRMS (ESI): calcd. for  $m/z$   $C_{29}H_{36}ClFN_8O_2$ ,  $[M + H]^+$  583.2706, found 583.2707. HPLC (80% methanol in water):  $t_R$  = 3.601 min, 97.46%.

**(3'-((5-Amino-6-chloropyrimidin-4-yl)amino)-2'-fluoro-4'-(4-methylpiperazin-1-yl)-[1,1'-biphenyl]-4-yl)(4-ethylpiperazin-1-yl)methanone (53).** The same procedure as that for 39. White solid, yield: 65%. mp 229–232 °C.  $^1H$  NMR (300 MHz, DMSO- $d_6$ ):  $\delta$  8.05 (s, 1H), 7.71 (s, 1H), 7.57 (d,  $J$  = 8.2 Hz, 2H), 7.47 (d,  $J$  = 8.1 Hz, 2H), 7.39 (t,  $J$  = 8.5 Hz, 2H), 7.00 (d,  $J$  = 8.7 Hz, 1H), 5.49 (s, 2H), 3.61 (s, 2H), 2.91 (s, 4H), 2.38–2.34 (m, 10H), 2.20 (s, 3H), 1.17 (t,  $J$  = 7.1 Hz, 2H), 1.01 (t,  $J$  = 7.1 Hz, 2H). HRMS (ESI): calcd. for  $m/z$   $C_{28}H_{34}ClFN_8O$ ,  $[M + H]^+$  553.2587, found 553.2596. HPLC (80% methanol in water):  $t_R$  = 3.794 min, 97.08%.

**N-(3'-((5-Amino-6-chloropyrimidin-4-yl)amino)-2'-fluoro-4'-(4-methylpiperazin-1-yl)-[1,1'-biphenyl]-4-yl)tetrahydro-2H-pyran-4-carboxamide (54).** The same procedure as that for 33. White solid, yield: 37%. mp >250 °C.  $^1H$  NMR (300 MHz, DMSO- $d_6$ ):  $\delta$  9.56 (s, 1H), 8.25 (s, 1H), 7.80–7.77 (m, 3H), 7.41–7.39 (m, 2H), 7.07 (dd,  $J$  = 7.5, 5.7 Hz, 1H), 6.68 (d,  $J$  = 7.3 Hz, 1H), 5.43 (s, 2H), 3.52–3.49 (m, 4H), 3.34 (t,  $J$  = 4.6 Hz, 4H), 2.70–2.67 (m, 1H), 2.44 (s, 4H), 2.22 (s, 3H), 2.06–1.99 (m, 2H), 1.85–1.78 (m, 2H). HRMS (ESI): calcd. for  $m/z$   $C_{27}H_{31}ClFN_7O_2$ ,  $[M + H]^+$  540.2285, found 540.2276. HPLC (90% methanol in water):  $t_R$  = 3.656 min, 98.94%.

**N-(3'-((5-Amino-6-chloropyrimidin-4-yl)amino)-2'-fluoro-4'-(4-methylpiperazin-1-yl)-[1,1'-biphenyl]-4-yl)-1-methylpiperidine-4-carboxamide (55).** The same procedure as that for 33. White solid, yield: 35%. mp >250 °C.  $^1H$  NMR (300 MHz, DMSO- $d_6$ ):  $\delta$  9.66 (s, 1H), 8.18 (s, 1H), 7.80 (s, 1H), 7.63 (d,  $J$  = 7.5 Hz, 2H), 7.40 (d,  $J$  = 7.6 Hz, 2H), 7.08–7.05 (m, 1H), 6.61 (d,  $J$  = 7.5 Hz, 1H), 5.30 (s, 2H), 3.20 (t,  $J$  = 4.9 Hz, 4H),

3.01–2.96 (m, 6H), 2.63–2.60 (m, 4H), 2.37 (s, 3H), 2.21–2.18 (m, 4H), 2.07–2.02 (m, 4H). HRMS (ESI): calcd. for  $m/z$   $C_{28}H_{34}ClFN_8O$ ,  $[M + H]^+$  553.2607, found 553.2606. HPLC (80% methanol in water):  $t_R$  = 3.168 min, 97.33%.

**N-(3'-((5-Amino-6-chloropyrimidin-4-yl)amino)-2'-fluoro-4'-(4-methylpiperazin-1-yl)-[1,1'-biphenyl]-4-yl)-2-(tetrahydro-2H-pyran-4-yl)acetamide (56).** The same procedure as that for 33. White solid, yield: 38.6%. mp >250 °C.  $^1H$  NMR (300 MHz, DMSO- $d_6$ ):  $\delta$  8.24 (s, 1H), 8.11 (s, 1H), 7.80 (s, 1H), 7.40 (s, 4H), 7.15–7.12 (m, 1H), 6.73 (d,  $J$  = 7.5 Hz, 1H), 5.42 (s, 2H), 3.55–3.50 (m, 4H), 3.53 (t,  $J$  = 4.6 Hz, 4H), 2.48 (s, 4H), 2.26 (s, 3H), 2.15 (d,  $J$  = 7.0 Hz, 2H), 2.03–2.01 (m, 1H), 1.70–1.64 (m, 4H). HRMS (ESI): calcd. for  $m/z$   $C_{28}H_{33}ClFN_7O_2$ ,  $[M + H]^+$  554.2441, found 554.2440. HPLC (80% methanol in water):  $t_R$  = 3.524 min, 99.10%.

**3'-((5-Amino-6-chloropyrimidin-4-yl)amino)-N,N, 2'-trimethyl-4'-(4-methylpiperazin-1-yl)-[1,1'-biphenyl]-4-carboxamide (57).** The same procedure as that for 54. White solid, yield: 44%. mp 165–167 °C.  $^1H$  NMR (300 MHz, DMSO- $d_6$ ):  $\delta$  8.09 (s, 1H), 7.87–7.85 (m, 2H), 7.80 (s, 1H), 7.58 (d,  $J$  = 7.4 Hz, 2H), 7.10 (d,  $J$  = 7.5 Hz, 1H), 6.86 (d,  $J$  = 7.5 Hz, 1H), 5.49 (s, 2H), 3.01–2.98 (m, 6H), 2.87 (s, 4H), 2.38 (s, 4H), 2.18 (s, 3H), 2.09 (s, 3H). (EI-MS):  $m/z$  480.2  $[M]^+$ . HPLC (80% methanol in water):  $t_R$  = 3.543 min, 96.37%.

**(5'-((5-Amino-6-chloropyrimidin-4-yl)amino)-2'-fluoro-4'-(4-methylpiperazin-1-yl)-[1,1'-biphenyl]-4-yl)-(morpholino)methanone (58).** The same procedure as that for 49. White solid, yield: 78%. mp 136–138 °C.  $^1H$  NMR (300 MHz, DMSO- $d_6$ ):  $\delta$  8.09 (s, 1H), 7.93 (d,  $J$  = 8.7 Hz, 1H), 7.82 (s, 1H), 7.59 (s, 2H), 7.51 (d,  $J$  = 7.8 Hz, 2H), 7.12 (d,  $J$  = 8.6 Hz, 1H), 5.40 (s, 2H), 3.61 (s, 4H), 2.97 (s, 4H), 2.72 (s, 4H), 2.54–2.51 (m, 4H), 2.41 (s, 3H). HRMS (ESI): calcd. for  $m/z$   $C_{26}H_{29}ClFN_7O_2$ ,  $[M + H]^+$  526.2128, found 526.2130. HPLC (80% methanol in water):  $t_R$  = 4.046 min, 96.85%.

**5'-((5-Amino-6-chloropyrimidin-4-yl)amino)-2'-fluoro-4'-(4-methylpiperazin-1-yl)-N-(2-morpholinoethyl)-[1,1'-biphenyl]-4-carboxamide (59).** The same procedure as that for 49. White solid, yield: 78%. mp 199–201 °C.  $^1H$  NMR (300 MHz, DMSO- $d_6$ ):  $\delta$  8.47 (s, 1H), 8.09 (s, 1H), 7.95–7.92 (m, 3H), 7.81 (s, 1H), 7.62 (d,  $J$  = 7.9 Hz, 2H), 7.11 (d,  $J$  = 12.4 Hz, 1H), 5.39 (s, 2H), 3.58 (t,  $J$  = 4.6 Hz, 4H), 3.41–3.40 (m, 4H), 2.92 (s, 4H), 2.56 (s, 4H), 2.45 (s, 4H), 2.29 (s, 3H). HRMS (ESI): calcd. for  $m/z$   $C_{28}H_{34}ClFN_8O_2$ ,  $[M + H]^+$  569.2550, found 569.2548. HPLC (80% methanol in water):  $t_R$  = 4.049 min, 98.64%.

**5'-((5-Amino-6-chloropyrimidin-4-yl)amino)-2'-fluoro-4'-(4-methylpiperazin-1-yl)-N-(3-morpholinopropyl)-[1,1'-biphenyl]-4-carboxamide (60).** The same procedure as that for 49. White solid, yield: 78%. mp 204–206 °C.  $^1H$  NMR (300 MHz, DMSO- $d_6$ ):  $\delta$  8.55 (s, 1H), 8.09 (s, 1H), 7.93–7.90 (m, 3H), 7.81 (s, 1H), 7.63–7.60 (m, 2H), 7.11 (d,  $J$  = 12.3 Hz, 1H), 5.39 (s, 2H), 3.59 (s, 4H), 3.32 (s, 4H), 2.92 (s, 4H), 2.58 (s, 4H), 2.41 (s, 4H), 2.31 (s, 3H), 1.72 (s, 2H). HRMS (ESI): calcd. for  $m/z$   $C_{29}H_{36}ClFN_8O_2$ ,  $[M + H]^+$  583.2693, found 583.2699. HPLC (80% methanol in water):  $t_R$  = 3.885 min, 99.38%.

**5'-((5-Amino-6-chloropyrimidin-4-yl)amino)-2'-fluoro-N-(4-hydroxycyclohexyl)-4'-(4-methylpiperazin-1-yl)-[1,1'-biphenyl]-4-carboxamide (61).** The same procedure as that for 49. White solid, yield: 65%. mp 200–203 °C.  $^1H$  NMR (300 MHz, DMSO- $d_6$ ):  $\delta$  9.67 (s, 1H), 8.06 (s, 1H), 7.92 (d,  $J$  = 8.4

H<sub>2</sub>, 1H), 7.82 (s, 1H), 7.58 (d, *J* = 7.7 Hz, 2H), 7.47 (d, *J* = 7.9 Hz, 2H), 7.21 (d, *J* = 12.2 Hz, 1H), 5.44 (s, 2H), 4.82 (s, 1H), 4.01 (s, 2H), 3.52 (s, 2H), 3.16 (s, 8H), 2.78 (s, 3H), 1.76 (s, 2H), 1.36 (s, 2H). HRMS (ESI): calcd. for *m/z* C<sub>27</sub>H<sub>31</sub>ClFN<sub>7</sub>O<sub>2</sub>, [M + H]<sup>+</sup> 554.2441, found 554.2442. HPLC (80% methanol in water): *t*<sub>R</sub> = 4.057 min, 98.48%.

**5'-((5-Amino-6-chloropyrimidin-4-yl)amino)-2'-fluoro-4'-(4-methylpiperazin-1-yl)-N-((tetrahydro-2H-pyran-4-yl)methyl)-[1,1'-biphenyl]-4-carboxamide (62).** The same procedure as that for 49. White solid, yield: 75%. mp 189–191 °C. <sup>1</sup>H NMR (300 MHz, DMSO-*d*<sub>6</sub>): δ 8.54 (s, 1H), 8.10 (s, 1H), 7.94–7.91 (m, 3H), 7.61 (d, *J* = 8.0 Hz, 2H), 7.11 (d, *J* = 12.2 Hz, 1H), 5.40 (s, 2H), 3.87–3.83 (m, 2H), 3.17 (s, 4H), 2.92 (s, 4H), 2.57 (s, 4H), 2.30 (s, 3H), 1.81 (s, 1H), 1.23 (s, 4H). HRMS (ESI): calcd. for *m/z* C<sub>28</sub>H<sub>33</sub>ClFN<sub>7</sub>O<sub>2</sub>, [M + H]<sup>+</sup> 540.2285, found 540.2284. HPLC (100% methanol): *t*<sub>R</sub> = 7.989 min, 99.16%.

**5'-((5-Amino-6-chloropyrimidin-4-yl)amino)-2'-fluoro-N,N-dimethyl-4'-(4-methylpiperazin-1-yl)-[1,1'-biphenyl]-4-carboxamide (63).** The same procedure as that for 49. White solid, yield: 75%. mp 157–159 °C. <sup>1</sup>H NMR (300 MHz, DMSO-*d*<sub>6</sub>): δ 8.01 (s, 1H), 7.83 (dd, *J* = 8.7, 3.7 Hz, 1H), 7.72 (d, *J* = 3.6 Hz, 1H), 7.49 (d, *J* = 7.1 Hz, 2H), 7.45–7.36 (m, 2H), 7.14–7.01 (m, 1H), 5.35 (s, 2H), 3.27–2.87 (m, 14H), 2.40 (s, 3H). <sup>13</sup>C NMR (75 MHz, DMSO-*d*<sub>6</sub>): δ 170.20, 157.23, 155.28, 150.61, 146.08, 145.70, 144.62, 139.76, 136.28, 136.08, 129.63, 128.86, 128.83, 127.87, 126.85, 125.39, 122.45, 108.70, 108.51, 54.04, 48.91, 35.26, 29.29, 22.57. HRMS (ESI): calcd. for *m/z* C<sub>24</sub>H<sub>27</sub>ClFN<sub>7</sub>O, [M + H]<sup>+</sup> 484.2022, found 484.2022. HPLC (80% methanol in water): *t*<sub>R</sub> = 4.751 min, 95.34%.

**5'-((5-Amino-6-chloropyrimidin-4-yl)amino)-2'-methyl-4'-(4-methylpiperazin-1-yl)-N-(3-morpholinopropyl)-[1,1'-biphenyl]-4-carboxamide (64).** The same procedure as that for 60, yield: 78%. mp 204–206 °C. <sup>1</sup>H NMR (300 MHz, DMSO-*d*<sub>6</sub>): δ 8.65 (s, 1H), 8.10 (s, 1H), 7.93–7.90 (m, 3H), 7.80 (s, 1H), 7.66–7.62 (m, 2H), 7.11 (d, *J* = 12.3 Hz, 1H), 5.39 (s, 2H), 3.59 (s, 4H), 3.32 (s, 4H), 2.92 (s, 4H), 2.58 (s, 4H), 2.41 (s, 4H), 2.31 (s, 6H), 1.72 (s, 2H). HRMS (ESI): calcd. for *m/z* C<sub>20</sub>H<sub>39</sub>ClN<sub>8</sub>O<sub>2</sub>, [M + H]<sup>+</sup> 579.2944, found 579.2950. HPLC (80% methanol in water): *t*<sub>R</sub> = 3.830 min, 98.82%.

**Molecular Docking.** The crystal structure of WDR5 (PDB 3SMR and 4QL1) was downloaded from the Protein Data Bank (PDB). All the compounds and protein structures were imported to Discovery Studio (DS) ver. 3.0, and the conformations were generated with the protocols “Prepare Protein” and “Prepare Ligands”, respectively. Molecular docking was performed using the CDocker tool, and the protein residues around the identified critical residues for WDR5-OICR-9429 were defined as the binding sites. The docking process was conducted with the default parameters unless otherwise mentioned. The high fitness score model was selected to analyze the binding model.

**Fluorescence Polarization Competition Assay.** The binding affinities of the synthesized compounds were tested using a fluorescence polarization (FP)-based competitive binding assay, which was described earlier.<sup>30,40,47</sup> The experimental buffer contained 100 mM KH<sub>2</sub>PO<sub>4</sub>, 25 mM KCl, and 0.01% Triton X-100 at pH 6.5. 10mer-Thr-FAM was used as a probe, and the reactions were performed in 384 black-well plates (no. 3575, Corning) with a total reaction volume of 60 μL (20 μL of the WDR5 protein, 20 μL of the

FAM-based probe, and 20 μL of the tested compounds). The FP assay ( $\lambda_{\text{ex}} = 485 \pm 25$  nm;  $\lambda_{\text{em}} = 535 \pm 25$  nm) was recorded using a SpectraMax GeminiXS (Molecular Devices, Sunnyvale, CA) instrument. The data were analyzed using GraphPad Prism ver. 6.0 software. IC<sub>50</sub> values represent three independent replicate determinations  $\pm$  the standard deviation.

**ITC Assay.** ITC (MicroCal iTC200) was used to determine the binding affinities between WDR5 and 63. Proteins with a concentration of 10 μM were prepared in the assay buffer (PBS buffer, pH 7.4) and subsequently injected into titration cells, and compounds with a concentration of 100 μM in the same assay buffer were in syringes. The whole injection procedure was set with intervals of 180 s and a stirring speed of 750 rpm and involved 19 injections in total. To prevent interference and ensure the accuracy, the first titration of the compound solution was 0.5 μL. Finally, Origin ver. 7.0 software was used to analyze the data obtained to determine the binding parameters, including the enthalpy value ( $\Delta H$ ), the entropy value ( $\Delta S$ ), and the association constant ( $K_a = 1/K_d$ ).

**In Vitro MLL HMT Functional Assay.** The MLL1 enzymatic reactions were conducted at room temperature for 60 min in a 50 μL mixture containing the methyltransferase assay buffer (50 mM HEPES, 100 mM NaCl, 1.0 mM EDTA, and 5% glycerol, pH 7.8), 1 μM (S)-adenosylmethionine (SAM), the MLL protein complex (MLL1/WDR5/ASH2/RbBP5/DPY30 = 1:1:1:1:1), and the test compound. These 50 μL reactions were carried out in the wells of a Histone substrate-precoated plate. Blocking buffer was added to stop the methylation reactions for 10 min. Then, 100 μL of the diluted primary antibody was added, and the mixture was slowly shaken for 60 min at room temperature. As before, the plate was emptied, washed three times, and shaken with blocking buffer for 10 min at room temperature. After discarding the blocking buffer, 100 μL of the diluted secondary antibody was added. The plate was then slowly shaken for 30 min at room temperature. As before, the plate was emptied, washed three times, and shaken with blocking buffer for 10 min at room temperature. The blocking buffer was discarded, and a mixture of the HRP chemiluminescent substrates was freshly prepared; 100 μL of this mixture was added to each empty well. Immediately, the luminescence of the samples was measured in a BioTek SynergyTM 2 microplate reader. The IC<sub>50</sub> values were calculated using nonlinear regression with a normalized dose–response fit using GraphPad Prism ver. 6.0 software. IC<sub>50</sub> values represent three independent replicate determinations  $\pm$  the standard deviation.

**AlphaScreen Assay.** To verify whether compound 63 had a good MLL1 HMT selectivity, the AlphaScreen assay was used to evaluate the compound's activity on other methyltransferases (G9a, Dot1L, EZH2, PRMT5, and SET8). The AlphaScreen IgG kit provides the necessary reagents for the test. The test was performed in a 384-well white plate (PerkinElmer). The buffer solution contained 10 mM PBS, compound 63, SAM, and proteins, and the solution was mixed at room temperature for 30 min. After the enzymatic reaction, 5 μL of receptor beads and 5 μL of the substrate antibodies were added to the reaction system, and the system was incubated for 30 min at room temperature. Then, 10 μL of AlphaScreen streptavidin-coupled donor beads were added. The 384-well white plate was investigated in an AlphaScreen microplate reader (EnSpire Alpha 2390 Multi-label Reader, PerkinElmer).



**In Vitro Antiproliferative Assay.** Antiproliferative activities of all the compounds against different cell lines were determined using the CCK8 assay kit. Cells were seeded as 3000–6000 cells per well in 96-well plates and treated with an inhibitor for 72 h at different concentrations in the culture medium. Cell viability was determined by the CCK8 kit (Beyotime, Jiangsu, China) according to the manufacturer's instructions.

**Western Blot Analysis.** Anti-H3K4me1 (ab8895), anti-H3K4me2 (ab32356), anti-H3K4me3 (ab8580), and anti-H3 (ab1791) were purchased from Abcam (Abcam, UK). The isolation of cell fractions and Western blotting were performed as detailed previously.<sup>28,35</sup> Briefly, the extracts were separated by SDS-PAGE and then electrotransferred to PVDF membranes (PerkinElmer, Northwalk, CT). Membranes were blocked with 1% BSA for 1 h, followed by incubation with a primary antibody at 4 °C overnight. Then, the membranes were washed and treated with a DyLight 800-labeled secondary antibody at 37 °C for 1 h. The membranes were screened through the odyssey infrared imaging system (LI-COR, Lincoln, NE).

**RNA Extraction and qRT-PCR Analysis.** The experimental procedure for quantitative real-time RT-PCR analysis was previously reported.<sup>35,47</sup> Briefly, the total RNA of MV4-11 cells was extracted from the treated cells using the TRIzol reagent (Invitrogen). Then, the RNA was converted to cDNA by reverse transcriptase (PrimeScript RT reagent kit) according to the manufacturer's instructions. Quantitative real-time RT-PCR analyses of *Hoxa9* and *Mes1* were performed by using the StepOne System Fast real-time PCR system (Applied Biosystems). The mRNA expression of all genes was normalized against the GAPDH expression.

**Cell Culture.** MV4-11, MOLM-13, K562, and HUVEC cell lines were purchased from the Cell Resource Center of Shanghai Institute for Biological Sciences, Chinese Academy of Sciences. The MV4-11 and K562 cells were cultured in a modified IMDM medium with 10% fetal bovine serum (FBS) and penicillin/streptomycin in a 37 °C incubator with 5% CO<sub>2</sub>. MOLM-13 cells were cultured in an RPMI-1640 medium supplemented with 10% (v/v) FBS. HUVEC cells were maintained in a modified DMEM medium that was supplemented with 10% FBS.

**Physicochemical Properties Experiments.** The distribution coefficients (CLogP) were computationally calculated using the ADMET Predictor 10.0 software. The permeability coefficients were determined via double-sink PAMPA on a PAMPA Explorer instrument (pION). The test compounds were diluted with the donor buffer at pH 7.4, placed in the donor side, and allowed to permeate to the acceptor side through the artificial membrane over 4 h of incubation at 25 °C. After incubation, the “sandwich” plate was separated. Then, the acceptor and donor solutions were each measured with a UV plate reader. Lastly, the permeability value was calculated by pION software.

**In Vitro Microsomal Stability Assay.** The metabolic stability of **63** was assessed using human and rat liver microsomes. **63** was preincubated with human and rat microsomes (0.7 mg/mL) at 1 μM for 5 min at 37 °C in PBS buffer (100 mM, pH 7.4) before 1 mM NADPH was added to initiate the reaction. Then, cold acetonitrile was utilized to precipitate the protein. Lastly, the samples were centrifuged for further analysis by LC-MS/MS.

**In Vivo Pharmacokinetic Assay.** Animal experiments were conducted according to protocols approved by the Institutional Animal Care and Use Committee of China Pharmaceutical University. Six healthy male SD rats, which were 6–8 weeks old and weighed 220 ± 30 g, were supplied by Joynn Laboratories. The rats (three for *p.o.* and three for *i.v.*) were administered with **63**. For *p.o.* administration, the test compound (10 mg/kg) was administered orally; for *i.v.* administration, the test compound (2 mg/kg) was administered intravenously. Blood samples were collected at times of 0, 0.0833, 0.25, 0.5, 1, 2, 4, 6, 8, and 24 h after administration for the *i.v.* group and at times of 0, 0.25, 0.5, 1, 2, 4, 6, 8, and 24 h after administration for the *p.o.* group. The resulting plasma samples were stored at –80 °C and analyzed by LC-MS/MS. Pharmacokinetic parameters shown are the mean ± SEM.

**In Vivo Antitumor Activity.** Animal experiments were conducted according to protocols approved by the Institutional Animal Care and Use Committee of China Pharmaceutical University. Six to eight week old female BALB/c nude mice were purchased from Shanghai Laboratory Animal Center, China Academy of Sciences, raised in air-conditioned rooms with 12 h of light per day, and fed with standard laboratory food and water. Approximately 5 × 10<sup>6</sup> MV4-11 cells suspended in PBS (0.2 mL) were injected into the flanks of nude mice. After the tumors grew to 100–150 mm<sup>3</sup>, all the mice were randomized into four groups (six mice for each group) and treated with the vehicle (0.9% saline solution) or compound **63** (40, 80, or 120 mg/kg) by oral administration daily for 21 days. Tumor volume and body weight were determined every other day by measuring the two perpendicular diameters of the tumors and using the formula  $V = \text{length (mm)} \times \text{width (mm)}^2 / 2$ . After 21 days of treatment, the mice were sacrificed, and the tumors were dissected and weighed. The drug efficacy was assessed by calculating the GI% =  $[1 - (TV_t - TV_0) / (CV_t - CT_0)] \times 100\%$ , where TV<sub>t</sub> and CV<sub>t</sub> are the tumor volume of treatments group and the control group measured at each time point, respectively, and TV<sub>0</sub> and CV<sub>0</sub> are the tumor volume of treatment group and the control group monitored at the beginning, respectively. The drug efficacy was also assessed by calculating TGI% =  $(\text{mean } W_{\text{control}} - \text{mean } W_{\text{tumor}}) / \text{mean } W_{\text{control}} \times 100\%$ .

## ■ ASSOCIATED CONTENT

### Supporting Information

The Supporting Information is available free of charge at <https://pubs.acs.org/doi/10.1021/acs.jmedchem.1c00091>.

Molecular formula strings (CSV)

Schematic diagram for targeting the WDR5–MLL1 PPI for the treatment of leukemia; docking study for compound **40**; and representative <sup>1</sup>H NMR, <sup>13</sup>C NMR, HRMS and HPLC spectra for the target compounds (PDF)

Dock study of compound **40** (PDB )

Dock study of compound **52** and **60** (PDB)

Dock study of compound **17** (PDB)

Dock study of compound **29** (PDB)

## AUTHOR INFORMATION

### Corresponding Authors

**Xiaoke Guo** – Jiangsu Key Laboratory of Drug Design and Optimization and State Key Laboratory of Natural Medicines and Department of Medicinal Chemistry, School of Pharmacy, China Pharmaceutical University, Nanjing 210009, China; [orcid.org/0000-0002-7558-5504](https://orcid.org/0000-0002-7558-5504); Email: [kexin95@126.com](mailto:kexin95@126.com)

**Qidong You** – Jiangsu Key Laboratory of Drug Design and Optimization and State Key Laboratory of Natural Medicines and Department of Medicinal Chemistry, School of Pharmacy, China Pharmaceutical University, Nanjing 210009, China; [orcid.org/0000-0002-8587-0122](https://orcid.org/0000-0002-8587-0122); Email: [youqd@163.com](mailto:youqd@163.com)

**Zhengyu Jiang** – Jiangsu Key Laboratory of Drug Design and Optimization and State Key Laboratory of Natural Medicines and Department of Medicinal Chemistry, School of Pharmacy, China Pharmaceutical University, Nanjing 210009, China; [orcid.org/0000-0002-1671-1582](https://orcid.org/0000-0002-1671-1582); Email: [jiangzhengyucpu@163.com](mailto:jiangzhengyucpu@163.com)

### Authors

**Weilin Chen** – Jiangsu Key Laboratory of Drug Design and Optimization and State Key Laboratory of Natural Medicines, China Pharmaceutical University, Nanjing 210009, China; Department of Medicinal Chemistry, School of Pharmacy, Nanjing Medical University, Nanjing 211166, China

**Xin Chen** – Jiangsu Key Laboratory of Drug Design and Optimization and State Key Laboratory of Natural Medicines, China Pharmaceutical University, Nanjing 210009, China

**Dongdong Li** – Jiangsu Key Laboratory of Drug Design and Optimization and State Key Laboratory of Natural Medicines, China Pharmaceutical University, Nanjing 210009, China

**Jianrui Zhou** – Jiangsu Key Laboratory of Drug Design and Optimization and State Key Laboratory of Natural Medicines, China Pharmaceutical University, Nanjing 210009, China

Complete contact information is available at:

<https://pubs.acs.org/10.1021/acs.jmedchem.1c00091>

### Author Contributions

<sup>†</sup>These authors contributed equally to this work.

### Notes

The authors declare no competing financial interest.

## ACKNOWLEDGMENTS

We are thankful for the financial support of the National Natural Science Foundation of China (nos. 81872799, 81930100, and 81773639), the Natural Science Foundation of Jiangsu Province of China (no. BK 20191321), Fundamental Research Funds for the Central Universities (no. 2632018ZD14), the National Science & Technology Major Project “Key New Drug Creation and Manufacturing Program” of China (2018ZX09711002), the Double First Class Innovation Team of China Pharmaceutical University (CPU2018GY02), the Program for Outstanding Scientific and Technological Innovation Team of Jiangsu Higher Education, the Open Project of State Key Laboratory of Natural Medicines (SKLNMZZCX201803), the Priority

Academic Program Development of Jiangsu Higher Education Institutions, and the Natural Science Research Project of Jiangsu Higher Education (20KJB350001).

## ABBREVIATIONS USED

ALL, acute lymphoid leukemia; AML, acute myeloid leukemia; FP, fluorescence polarization; GI, growth inhibition; HMT, histone methyltransferase; H3K4, histone 3 lysine 4; ITC, isothermal titration calorimetry; MLL1, mixed lineage leukemia 1; PPI, protein–protein interaction; TGI, tumor weight growth inhibition; WBM, WDR5 binding motif; WDR5, WD repeat-containing protein 5; WIN, WDR5 interaction motif

## REFERENCES

- (1) Stirnimann, C. U.; Petsalaki, E.; Russell, R. B.; Müller, C. W. WD40 Proteins Propel Cellular Networks. *Trends Biochem. Sci.* **2010**, *35*, 565–574.
- (2) Xu, C.; Min, J. Structure and Function of WD40 Domain Proteins. *Protein Cell* **2011**, *2*, 202–214.
- (3) Guarnaccia, A. D.; Tansey, W. P. Moonlighting with WDR5: A Cellular Multitasker. *J. Clin. Med.* **2018**, *7*, 21.
- (4) Trievel, R. C.; Shilatifard, A. WDR5, a complexed protein. *Nat. Struct. Mol. Biol.* **2009**, *16*, 678–680.
- (5) Patel, A.; Vought, V. E.; Dharmarajan, V.; Cosgrove, M. S. A conserved arginine-containing motif crucial for the assembly and enzymatic activity of the mixed lineage leukemia protein-1 core complex. *J. Biol. Chem.* **2008**, *283*, 32162–32175.
- (6) Odho, Z.; Southall, S. M.; Wilson, J. R. Characterization of a novel WDR5-binding site that recruits RbBP5 through a conserved motif to enhance methylation of histone H3 lysine 4 by mixed lineage leukemia protein-1. *J. Biol. Chem.* **2010**, *285*, 32967–32976.
- (7) Carugo, A.; Genovese, G.; Seth, S.; Nezi, L.; Rose, J. L.; Bossi, D.; Cicalese, A.; Shah, P. K.; Viale, A.; Pettazzoni, P. F.; Akdemir, K. C.; Bristow, C. A.; Robinson, F. S.; Tepper, J.; Sanchez, N.; Gupta, S.; Estecio, M. R.; Giuliani, V.; Dellino, G. I.; Riva, L.; Yao, W.; Di Francesco, M. E.; Green, T.; D'Alesio, C.; Corti, D.; Kang, Y.; Jones, P.; Wang, H.; Fleming, J. B.; Maitra, A.; Pelicci, P. G.; Chin, L.; DePinho, R. A.; Lanfrancone, L.; Heffernan, T. P.; Draetta, G. F. In Vivo Functional Platform Targeting Patient-Derived Xenografts Identifies WDR5-MYC Association as a Critical Determinant of Pancreatic Cancer. *Cell Rep.* **2016**, *16*, 133–147.
- (8) Thomas, L. R.; Adams, C. M.; Fesik, S. W.; Eischen, C. M.; Tansey, W. P. Targeting MYC through WDR5. *Mol. Cell Oncol.* **2020**, *7*, 1709388.
- (9) Thomas, L. R.; Wang, Q.; Grieb, B. C.; Phan, J.; Foshage, A. M.; Sun, Q.; Olejniczak, E. T.; Clark, T.; Dey, S.; Lorey, S.; Alicie, B.; Howard, G. C.; Cawthon, B.; Ess, K. C.; Eischen, C. M.; Zhao, Z.; Fesik, S. W.; Tansey, W. P. Interaction with WDR5 promotes target gene recognition and tumorigenesis by MYC. *Mol. Cell* **2015**, *58*, 440–452.
- (10) Macdonald, J. D.; Chacon Simon, S.; Han, C.; Wang, F.; Shaw, J. G.; Howes, J. E.; Sai, J.; Yuh, J. P.; Camper, D.; Alicie, B. M.; Alvarado, J.; Nikhar, S.; Payne, W.; Aho, E. R.; Bauer, J. A.; Zhao, B.; Phan, J.; Thomas, L. R.; Rossanese, O. W.; Tansey, W. P.; Waterson, A. G.; Stauffer, S. R.; Fesik, S. W. Discovery and Optimization of Salicylic Acid-Derived Sulfonamide Inhibitors of the WD Repeat-Containing Protein 5-MYC Protein-Protein Interaction. *J. Med. Chem.* **2019**, *62*, 11232–11259.
- (11) Chacon Simon, S.; Wang, F.; Thomas, L. R.; Phan, J.; Zhao, B.; Olejniczak, E. T.; Macdonald, J. D.; Shaw, J. G.; Schlund, C.; Payne, W.; Creighton, J.; Stauffer, S. R.; Waterson, A. G.; Tansey, W. P.; Fesik, S. W. Discovery of WD Repeat-Containing Protein 5 (WDR5)-MYC Inhibitors Using Fragment-Based Methods and Structure-Based Design. *J. Med. Chem.* **2020**, *63*, 4315–4333.



- (12) Crawford, B. D.; Hess, J. L. MLL core components give the green light to histone methylation. *ACS Chem. Biol.* **2006**, *1*, 495–498.
- (13) Patel, A.; Dharmarajan, V.; Cosgrove, M. S. Structure of WDR5 bound to mixed lineage leukemia protein-1 peptide. *J. Biol. Chem.* **2008**, *283*, 32158–32161.
- (14) Song, J. J.; Kingston, R. E. WDR5 interacts with mixed lineage leukemia (MLL) protein via the histone H3-binding pocket. *J. Biol. Chem.* **2008**, *283*, 35258–35264.
- (15) Dou, Y.; Milne, T. A.; Ruthenburg, A. J.; Lee, S.; Lee, J. W.; Verdine, G. L.; Allis, C. D.; Roeder, R. G. Regulation of MLL1 H3K4 methyltransferase activity by its core components. *Nat. Struct. Mol. Biol.* **2006**, *13*, 713–719.
- (16) Hess, J. L. MLL: A Histone Methyltransferase Disrupted in Leukemia. *Trends Mol. Med.* **2004**, *10*, 500–507.
- (17) Muntean, A. G.; Hess, J. L. The Pathogenesis of Mixed-Lineage Leukemia. *Annu. Rev. Pathol.: Mech. Dis.* **2012**, *7*, 283–301.
- (18) Winters, A. C.; Bernt, K. M. MLL-Rearranged Leukemias-An Update on Science and Clinical Approaches. *Front Pediatr.* **2017**, *5*, 4.
- (19) Krivtsov, A. V.; Armstrong, S. A. MLL Translocations, Histone Modifications and Leukaemia Stem-Cell Development. *Nat. Rev. Cancer* **2007**, *7*, 823–833.
- (20) Thiel, A. T.; Blessington, P.; Zou, T.; Feather, D.; Wu, X.; Yan, J.; Zhang, H.; Liu, Z.; Ernst, P.; Koretzky, G. A.; Hua, X. MLL-AF9-Induced leukemogenesis requires coexpression of the wild-type Mll allele. *Cancer Cell* **2010**, *17*, 148–159.
- (21) Milne, T. A.; Kim, J.; Wang, G. G.; Stadler, S. C.; Basrur, V.; Whitcomb, S. J.; Wang, Z.; Ruthenburg, A. J.; Elenitoba-Johnson, K. S. J.; Roeder, R. G.; Allis, C. D. Multiple interactions recruit MLL1 and MLL1 fusion proteins to the HOXA9 locus in leukemogenesis. *Mol. Cell* **2010**, *38*, 853–863.
- (22) Wang, Z. H.; Li, D. D.; Chen, W. L.; You, Q. D.; Guo, X. K. Targeting protein-protein interaction between MLL1 and reciprocal proteins for leukemia therapy. *Bioorg. Med. Chem.* **2018**, *26*, 356–365.
- (23) Karatas, H.; Townsend, E. C.; Bernard, D.; Dou, Y.; Wang, S. Analysis of the binding of mixed lineage leukemia 1 (MLL1) and histone 3 peptides to WD repeat domain 5 (WDR5) for the design of inhibitors of the MLL1-WDR5 interaction. *J. Med. Chem.* **2010**, *53*, 5179–5185.
- (24) Karatas, H.; Townsend, E. C.; Cao, F.; Chen, Y.; Bernard, D.; Liu, L.; Lei, M.; Dou, Y.; Wang, S. High-Affinity, Small-Molecule Peptidomimetic Inhibitors of MLL1/WDR5 Protein-Protein Interaction. *J. Am. Chem. Soc.* **2013**, *135*, 669–682.
- (25) Cao, F.; Townsend, E. C.; Karatas, H.; Xu, J.; Li, L.; Lee, S.; Liu, L.; Chen, Y.; Ouillet, P.; Zhu, J.; Hess, J. L.; Atadja, P.; Lei, M.; Qin, Z. S.; Malek, S.; Wang, S.; Dou, Y. Targeting MLL1 H3K4 methyltransferase activity in mixed-lineage leukemia. *Mol. Cell* **2014**, *53*, 247–261.
- (26) Karatas, H.; Li, Y.; Liu, L.; Ji, J.; Lee, S.; Chen, Y.; Yang, J.; Huang, L.; Bernard, D.; Xu, J.; Townsend, E. C.; Cao, F.; Ran, X.; Li, X.; Wen, B.; Sun, D.; Stuckey, J. A.; Lei, M.; Dou, Y.; Wang, S. Discovery of a highly potent, cell-permeable macrocyclic peptidomimetic (MM-589) targeting the WD repeat domain 5 protein (WDR5)-mixed lineage leukemia (MLL) protein-protein interaction. *J. Med. Chem.* **2017**, *60*, 4818–4839.
- (27) Senisterra, G.; Wu, H.; Allali-Hassani, A.; Wasney, G. A.; Barsyte-Lovejoy, D.; Dombrowski, L.; Dong, A.; Nguyen, K. T.; Smil, D.; Bolshan, Y.; Hajian, T.; He, H.; Seitova, A.; Chau, I.; Li, F.; Poda, G.; Couture, J. F.; Brown, P. J.; Al-Awar, R.; Schapira, M.; Arrowsmith, C. H.; Vedadi, M. Small-molecule inhibition of MLL1 activity by disruption of its interaction with WDR5. *Biochem. J.* **2013**, *449*, 151–159.
- (28) Grebien, F.; Vedadi, M.; Getlik, M.; Giambro, R.; Grover, A.; Avellino, R.; Skucha, A.; Vittori, S.; Kuznetsova, E.; Smil, D.; Barsyte-Lovejoy, D.; Li, F.; Poda, G.; Schapira, M.; Wu, H.; Dong, A.; Senisterra, G.; Stukalov, A.; Huber, K. V. M.; Schonegger, A.; Marcellus, R.; Bilban, M.; Bock, C.; Brown, P. J.; Zuber, J.; Bennett, K. L.; Al-Awar, R.; Delwel, R.; Nerlov, C.; Arrowsmith, C. H.; Superti-Furga, G. Pharmacological targeting of the WDR5-MLL interaction in C/EBP $\alpha$  N-terminal leukemia. *Nat. Chem. Biol.* **2015**, *11*, 571–578.
- (29) Getlik, M.; Smil, D.; Zepeda-Velazquez, C.; Bolshan, Y.; Poda, G.; Wu, H.; Dong, A.; Kuznetsova, E.; Marcellus, R.; Senisterra, G.; Dombrowski, L.; Hajian, T.; Kiyota, T.; Schapira, M.; Arrowsmith, C. H.; Brown, P. J.; Vedadi, M.; Al-Awar, R. Structure-based optimization of a small molecule antagonist of the interaction between WD repeat-containing protein 5 (WDR5) and mixed-lineage leukemia 1 (MLL1). *J. Med. Chem.* **2016**, *59*, 2478–2496.
- (30) Li, D. D.; Chen, W. L.; Wang, Z. H.; Xie, Y. Y.; Xu, X. L.; Jiang, Z. Y.; Zhang, X. J.; You, Q. D.; Guo, X. K. High-affinity small molecular blockers of mixed lineage leukemia 1 (MLL1)-WDR5 interaction inhibit MLL1 complex H3K4 methyltransferase activity. *Eur. J. Med. Chem.* **2016**, *124*, 480–489.
- (31) Wang, F.; Jeon, K. O.; Salovich, J. M.; Macdonald, J. D.; Alvarado, J.; Gogliotti, R. D.; Phan, J.; Olejniczak, E. T.; Sun, Q.; Wang, S.; Camper, D.; Yuh, J. P.; Shaw, J. G.; Sai, J.; Rossanese, O. W.; Tansey, W. P.; Stauffer, S. R.; Fesik, S. W. Discovery of Potent 2-Aryl-6,7-Dihydro-5 H-Pyrrolo[1,2-*a*]imidazoles as WDR5 WIN-site Inhibitors Using Fragment-Based Methods and Structure-Based Design. *J. Med. Chem.* **2018**, *61*, 5623–5642.
- (32) Tian, J.; Teuscher, K. B.; Aho, E. R.; Alvarado, J. R.; Mills, J. J.; Meyers, K. M.; Gogliotti, R. D.; Han, C.; Macdonald, J. D.; Sai, J.; Shaw, J. G.; Sensintaffar, J. L.; Zhao, B.; Rietz, T. A.; Thomas, L. R.; Payne, W. G.; Moore, W. J.; Stott, G. M.; Kondo, J.; Inoue, M.; Coffey, R. J.; Tansey, W. P.; Stauffer, S. R.; Lee, T.; Fesik, S. W. Discovery and Structure-Based Optimization of Potent and Selective WD Repeat Domain 5 (WDR5) Inhibitors Containing a Dihydroisoquinolinone Bicyclic Core. *J. Med. Chem.* **2020**, *63*, 656–675.
- (33) Aho, E. R.; Wang, J.; Gogliotti, R. D.; Howard, G. C.; Phan, J.; Acharya, P.; Macdonald, J. D.; Cheng, K.; Lorey, S. L.; Lu, B.; Wenzel, S.; Foshage, A. M.; Alvarado, J.; Wang, F.; Shaw, J. G.; Zhao, B.; Weissmiller, A. M.; Thomas, L. R.; Vakoc, C. R.; Hall, M. D.; Hiebert, S. W.; Liu, Q.; Stauffer, S. R.; Fesik, S. W.; Tansey, W. P. Displacement of WDR5 from Chromatin by a WIN Site Inhibitor with Picomolar Affinity. *Cell Rep.* **2019**, *26*, 2916–2928.
- (34) Aeluri, M.; Chamakuri, S.; Dasari, B.; Guduru, S. K.; Jimmidi, R.; Jogula, S.; Arya, P. Small molecule modulators of protein-protein interactions: selected case studies. *Chem. Rev.* **2014**, *114*, 4640–4694.
- (35) Arkin, M. R.; Tang, Y.; Wells, J. A. Small-molecule inhibitors of protein-protein interactions: progressing toward the reality. *Chem. Biol.* **2014**, *21*, 1102–1114.
- (36) Janzen, W. P. Screening technologies for small molecule discovery: the state of the art. *Chem. Biol.* **2014**, *21*, 1162–1170.
- (37) Lawson, A. D. G.; MacCoss, M.; Heer, J. P. Importance of Rigidity in Designing Small Molecule Drugs To Tackle Protein-Protein Interactions (PPIs) through Stabilization of Desired Conformers. *J. Med. Chem.* **2018**, *61*, 4283–4289.
- (38) Wang, L.; Zhang, L. X.; Li, L.; Jiang, J. S.; Zheng, Z.; Shang, J. L.; Wang, C. X.; Chen, W. L.; Bao, Q. C.; Xu, X. L.; Jiang, Z. Y.; Zhang, J.; You, Q. D. Small-molecule inhibitor targeting the Hsp90-Cdc37 protein-protein interaction in colorectal cancer. *Sci. Adv.* **2019**, *5*, eaax2277.
- (39) Bolshan, Y.; Getlik, M.; Kuznetsova, E.; Wasney, G. A.; Hajian, T.; Poda, G.; Nguyen, K. T.; Wu, H.; Dombrowski, L.; Dong, A.; Senisterra, G.; Schapira, M.; Arrowsmith, C. H.; Brown, P. J.; Al-Awar, R.; Vedadi, M.; Smil, D. Synthesis, Optimization, and Evaluation of Novel Small Molecules as Antagonists of WDR5-MLL Interaction. *ACS Med. Chem. Lett.* **2013**, *4*, 353–357.
- (40) Li, D. D.; Chen, W. L.; Xu, X. L.; Jiang, J. S.; Xie, Y. Y.; Zhang, X. J.; Guo, X. K.; You, Q. D.; Sun, H. P. Structure-based design and synthesis of small molecular inhibitors disturbing the interaction of MLL1-WDR5. *Eur. J. Med. Chem.* **2016**, *118*, 1–8.
- (41) Artinger, E. L.; Mishra, B. P.; Zaffuto, K. M.; Li, B. E.; Chung, E. K.; Moore, A. W.; Chen, Y.; Cheng, C.; Ernst, P. An MLL-dependent network sustains hematopoiesis. *Proc. Natl. Acad. Sci. U. S. A.* **2013**, *110*, 12000–12005.

(42) Jude, C. D.; Climer, L.; Xu, D.; Artinger, E.; Fisher, J. K.; Ernst, P. Unique and independent roles for MLL in adult hematopoietic stem cells and progenitors. *Cell Stem Cell* **2007**, *1*, 324–337.

(43) McMahon, K. A.; Hiew, S. Y.; Hadjur, S.; Veiga-Fernandes, H.; Menzel, U.; Price, A. J.; Kioussis, D.; Williams, O.; Brady, H. J. MLL has a critical role in fetal and adult hematopoietic stem cell self-renewal. *Cell Stem Cell* **2007**, *1*, 338–345.

(44) Yu, B. D.; Hess, J. L.; Horning, S. E.; Brown, G. A.; Korsmeyer, S. J. Altered Hox expression and segmental identity in Mll-mutant mice. *Nature* **1995**, *378*, 505–508.

(45) Lim, D. A.; Huang, Y. C.; Swigut, T.; Mirick, A. L.; Garcia-Verdugo, J. M.; Wysocka, J.; Ernst, P.; Alvarez-Buylla, A. Chromatin remodelling factor MLL1 is essential for neurogenesis from postnatal neural stem cells. *Nature* **2009**, *458*, 529–533.

(46) Alicea-Velázquez, N. L.; Shinsky, S. A.; Loh, D. M.; Lee, J.-H.; Skalniak, D. G.; Cosgrove, M. S. Targeted Disruption of the Interaction between WD-40 Repeat Protein 5 (WDR5) and Mixed Lineage Leukemia (MLL)/SET1 Family Proteins Specifically Inhibits MLL1 and SETD1A Methyltransferase Complexes. *J. Biol. Chem.* **2016**, *291*, 22357–22372.

(47) Li, D. D.; Wang, Z. H.; Chen, W. L.; Xie, Y. Y.; You, Q. D.; Guo, X. K. Structure-based design of ester compounds to inhibit MLL complex catalytic activity by targeting mixed lineage leukemia 1 (MLL1)-WDR5 interaction. *Bioorg. Med. Chem.* **2016**, *24*, 6109–6118.

#### ■ NOTE ADDED AFTER ASAP PUBLICATION

Published ASAP on June 9, 2021; Table 5 revised on June 14, 2021.